



Effects of thermal expansion on moderately intense turbulence in premixed flames

Downloaded from: <https://research.chalmers.se>, 2024-03-13 07:46 UTC

Citation for the original published paper (version of record):

Sabelnikov, V., Lipatnikov, A., Nikitin, N. et al (2022). Effects of thermal expansion on moderately intense turbulence in premixed flames. *Physics of Fluids*, 34(11).
<http://dx.doi.org/10.1063/5.0123211>

N.B. When citing this work, cite the original published paper.

Effects of thermal expansion on moderately intense turbulence in premixed flames

Vladimir A. Sabelnikov^{a,b}, Andrei N. Lipatnikov^{c,*}, Nikolay V. Nikitin^d, Francisco E. Hernández-Pérez^e, Hong G. Im^e

^aONERA – The French Aerospace Laboratory, F-91761 Palaiseau, France

^bCentral Aerohydrodynamic Institute (TsAGI), 140180 Zhukovsky, Moscow Region, Russian Federation

^cDepartment of Mechanics and Maritime Sciences, Chalmers University of Technology, Gothenburg, 41296 Sweden

^dLomonosov Moscow State University, Moscow, Russian Federation

^eClean Combustion Research Center, King Abdullah University of Science and Technology, Thuwal 23955-6900, Saudi Arabia

*Corresponding author, lipatn@chalmers.se

Abstract

The study aims at analytically and numerically exploring the influence of combustion-induced thermal expansion on turbulence in premixed flames. In the theoretical part, contributions of solenoidal and potential velocity fluctuations to the unclosed component of the advection term in the Reynolds-averaged Navier-Stokes equations are compared and a new criterion for assessing the importance of the thermal expansion effects is introduced. The criterion highlights a ratio of the dilatation in the laminar flame to the large-scale gradient of root-mean-square (rms) velocity in the turbulent flame brush. To support the theoretical study, direct numerical simulation (DNS) data obtained earlier from two complex-chemistry, lean H₂-air flames are analyzed. In line with the new criterion, even at sufficiently high Karlovitz numbers, results show significant influence of combustion-induced potential velocity fluctuations on the second moments of the turbulent velocity upstream of and within the flame brush. In particular, the DNS data demonstrate that (i) potential and solenoidal rms velocities are comparable in the unburnt gas close to the leading edge of the flame brush and (ii) potential and solenoidal rms velocities conditioned to unburnt gas are comparable within the entire flame brush. Moreover, combustion-induced thermal expansion affects not only the potential velocity, but even the solenoidal one. The latter effects manifest themselves in a negative correlation between solenoidal velocity fluctuations and dilatation or in the counter-gradient behavior of the solenoidal scalar flux. Finally, a turbulence-in-premixed-flame diagram is sketched to discuss the influence of combustion-induced thermal expansion on various ranges of turbulence spectrum.

I. INTRODUCTION

Since the pioneering work by Karlovitz et al.¹ and Libby and Bray,² effects of thermal expansion on turbulence (e.g., so-called flame-generated turbulence¹) and turbulent scalar transport (e.g., so-called counter-gradient diffusion²) in premixed flames have long been a challenging research subject.³⁻¹⁵ Numerical studies reviewed elsewhere¹⁶⁻¹⁹ indicate that the influence of combustion-induced thermal expansion on turbulence within a premixed flame brush is well (hardly) pronounced in weakly (highly) turbulent flames. Recent Direct Numerical Simulation^{11,20-23} (DNS) and experimental^{24,25} investigations further support this view. However, criteria for finding domains of importance of such an influence have not yet been well established.

One of the widely accepted criteria of this kind was suggested by Bray²⁶ who considered turbulent scalar transport to be counter-gradient if

$$N_B = \frac{(\sigma-1)S_L}{2\alpha u'} > 1. \quad (1)$$

Here, $\sigma = \rho_u/\rho_b$ is the density ratio; S_L is the laminar flame speed; u' is root-mean-square (rms) turbulent velocity; subscript u or b designates unburnt or burnt mixture, respectively; and the number N_B is known as Bray number. The factor α is of unity order and is expected to increase with increasing a ratio of an integral length scale L of turbulence to the laminar flame thickness δ_L .²⁷ Since a widely accepted model of α has not yet been developed, this factor is often omitted in Eq. (1). In any case, turbulent scalar transport is not the major subject of the present study, which is rather focused on the influence of combustion-induced thermal expansion on the second moments of the turbulent velocity field.

By considering the influence of combustion-induced thermal expansion on small-scale turbulent eddies, Bilger²⁸ has hypothesized that such an influence is significant if the magnitude τ_K^{-1} of velocity gradients in the smallest eddies is less than dilation $\Theta = (\sigma - 1)\tau_f^{-1}$ in the laminar flame. Therefore, the following criterion should hold

$$Ka < Ka_{cr}^B = \sigma - 1 \quad (2)$$

in order for the influence of combustion-induced thermal expansion on small-scale turbulent eddies to be substantial. Here, $Ka = \tau_f/\tau_K$ designates Karlovitz number; $\tau_f = \delta_L/S_L$ and $\tau_K = \eta_K/u_K = (\nu_u/\bar{\epsilon})^{1/2}$ are the laminar flame and Kolmogorov time scales, respectively; $u_K = (\nu_u\bar{\epsilon})^{1/4}$ and $\eta_K = (\nu_u^3/\bar{\epsilon})^{1/4}$ are Kolmogorov velocity and length scales²⁵, respectively; ν is the kinematic viscosity of unburnt mixture; $\bar{\epsilon} = 2\nu\overline{S_{jk}S_{jk}}$ is a mean dissipation rate; $S_{jk} = 0.5(\partial u_j/\partial x_k + \partial u_k/\partial x_j)$ is the rate-of-strain tensor; and summation convention applies to repeated indices. Note that (i) under conditions of a low Mach number, as in the case under study, dilatational contribution to the mean dissipation rate is commonly neglected if turbulence characteristics in Ka are evaluated in the incompressible flow of unburnt reactants; and (ii) to properly characterize the dilatation magnitude, the laminar flame thickness should be evaluated as follows: $\delta_L = (T_b - T_u)/\max|\nabla T|$, where T is the temperature. The simple criterion given by Eq. (2) was recently supported in a DNS study^{30,31} of two stoichiometric H₂-air jet turbulent flames characterized by $Ka = 3.7 < Ka_{cr}^B = 6.7$ and $Ka = 54 > Ka_{cr}^B$.

Besides the influence of combustion-induced thermal expansion on the smallest turbulent eddies, addressed by Bilger,²⁸ larger eddies from the inertial range of Kolmogorov turbulence²⁹ may also be affected by the thermal expansion in flames.^{10,32} In particular, O'Brien et al.³² have theorized that thermal energy released by combustion and transformed

76 to kinetic energy at small scales can be transferred via inverse turbulence cascade to larger
 77 eddies (this phenomenon is known as backscatter) whose time scale is shorter than or equal
 78 to τ_f . MacArt and Mueller¹⁰ have also argued that “competition between a heat-release-
 79 induced cascade and the classical, production-driven forward cascade” can appear under
 80 certain conditions even if $Ka > Ka_{cr}^B$.

81 As far as the largest turbulent eddies, whose length scale is on the order of L , are concerned,
 82 the present authors are not aware of a criterion characterizing the influence of combustion-
 83 induced thermal expansion on such eddies. This work aims primarily at bridging this
 84 knowledge gap.

85 In Sect. II, a new criterion is introduced by analyzing contributions of potential and
 86 solenoidal components of a fluctuating velocity field to various terms in transport equations
 87 for turbulent Reynolds stresses. To support this theoretical analysis, such potential and
 88 solenoidal contributions are explored by processing published DNS data described briefly in
 89 Sect. III. Results are reported in Sect. IV. The newly proposed criterion is compared with
 90 other relevant criteria in Sect. V, where a simple diagram is drawn to speculate what ranges
 91 of turbulence spectrum are substantially affected by combustion-induced thermal expansion
 92 in a premixed flame under various conditions. Conclusions are summarized in Sect. VI.

93 It is worth stressing that (i) the newly introduced criterion complements criteria suggested
 94 earlier, e.g., Eq. (2), rather than replacing them and (ii) another effect of combustion on
 95 turbulence, i.e., turbulence decay due to an increase in kinematic viscosity with the
 96 temperature, is not explored in the present paper, while this mechanism is considered in the
 97 DNS discussed in Sects. III and IV.

98 II. A THEORETICAL ANALYSIS

99 A. Reynolds-average framework

100 Let us consider the Reynolds-averaged Navier-Stokes equations written in a non-
101 conservative form:

$$102 \quad \frac{\partial \bar{u}_i}{\partial t} + \bar{u}_k \frac{\partial \bar{u}_i}{\partial x_k} + \overline{u'_k \frac{\partial u'_i}{\partial x_k}} = -\frac{1}{\rho} \frac{\partial \bar{p}}{\partial x_i} + \frac{1}{\rho} \frac{\partial \tau_{ik}}{\partial x_k}. \quad (3)$$

103 Here, $u_i = \bar{u}_i + u'_i$ is i -th component of the velocity vector $\mathbf{u} = \bar{\mathbf{u}} + \mathbf{u}'$; t designates time; x_i
104 are Cartesian coordinates; p is the pressure; τ_{ik} is the viscous stress tensor; and overbars
105 designate Reynolds averages.

106 For constant-density flows, turbulence models aim at closing the Reynolds stresses $\overline{u'_i u'_k}$ or
107 the last term on the left-hand side (LHS) of Eq. (3). Moreover, in constant-density turbulence
108 in an unbounded domain, $\mathbf{u}'(\mathbf{x}, t)$ stems from a solenoidal (rotational) motion and $\nabla \cdot \mathbf{u}' = 0$.
109 In flames, $\nabla \cdot \mathbf{u}' \neq 0$ due to thermal expansion, with combustion-induced pressure
110 perturbations creating potential (irrotational) velocity fluctuations. Thus, eventual importance
111 of combustion-induced thermal expansion effects could be assessed by comparing
112 contributions of solenoidal and potential velocity fields to major turbulence characteristics. In
113 the following, this task is pursued by examining the last term on the LHS of Eq. (3).

114 If one performs a Helmholtz-Hodge decomposition (HHD) of the velocity field $\mathbf{u}'(\mathbf{x}, t)$ into
115 divergence-free solenoidal and irrotational potential fields, $\mathbf{u}'_s(\mathbf{x}, t)$ and $\mathbf{u}'_p(\mathbf{x}, t)$, respectively,
116 the following equations hold³³

$$117 \quad u'_i = u'_{s,i} + u'_{p,i}; \quad \frac{\partial u'_{s,k}}{\partial x_k} = 0; \quad \frac{\partial u'_{p,k}}{\partial x_i} = \frac{\partial u'_{p,i}}{\partial x_k}. \quad (4)$$

118 The last equality results directly from $\nabla \times \mathbf{u}'_p = 0$. Substitution of Eqs. (4) into the last term
119 on the LHS of Eq. (3) yields

$$\begin{aligned} 120 \quad \overline{u'_k \frac{\partial u'_l}{\partial x_k}} &= \overline{u'_{s,k} \frac{\partial u'_{s,l}}{\partial x_k}} + \overline{u'_{s,k} \frac{\partial u'_{p,l}}{\partial x_k}} + \overline{u'_{p,k} \frac{\partial u'_{s,l}}{\partial x_k}} + \overline{u'_{p,k} \frac{\partial u'_{p,l}}{\partial x_k}} \\ 121 \quad &= \frac{\partial \overline{u'_{s,l} u'_{s,k}}}{\partial x_k} + \frac{\partial \overline{u'_{p,l} u'_{s,k}}}{\partial x_k} + \frac{\partial \overline{u'_{p,k} u'_{s,l}}}{\partial x_k} - \overline{u'_{s,l} \frac{\partial u'_{p,k}}{\partial x_k}} + \overline{u'_{p,k} \frac{\partial u'_{p,l}}{\partial x_l}} \\ 122 \quad &= \frac{\partial}{\partial x_k} (\overline{u'_{s,l} u'_{s,k}} + \overline{u'_{p,l} u'_{s,k}} + \overline{u'_{s,l} u'_{p,k}}) + \frac{1}{2} \frac{\partial}{\partial x_l} \overline{u'_{p,k} u'_{p,k}} - \overline{u'_{s,l} \frac{\partial u'_{p,k}}{\partial x_k}}. \end{aligned} \quad (5)$$

123 The last term in the second line of Eq. (5) results from substitution of the last equality in Eq.
124 (4) into the last term in the first line of Eq. (5).

125 In the simplest statistically one-dimensional (1D) and planar case, Eq. (5) reads

$$126 \quad \overline{u'_k \frac{\partial u'_l}{\partial x_k}} = \underbrace{\frac{\partial \overline{u'^2_{s,1}}}{\partial x_1}}_{T_1} + 2 \underbrace{\frac{\partial \overline{u'_{s,1} u'_{p,1}}}{\partial x_1}}_{T_2} + \underbrace{\frac{1}{2} \frac{\partial \overline{u'^2_{p,k} u'_{p,k}}}{\partial x_1}}_{T_3} - \underbrace{u'_{s,1} \frac{\partial u'_{p,k}}{\partial x_k}}_{T_4}. \quad (6)$$

127 Close to a boundary of importance of the studied thermal expansion effects, the order of
128 magnitude of the potential velocity fluctuations cannot be larger than the order of magnitude
129 of the rotational velocity fluctuations. Accordingly, within the mean flame brush, the order of
130 magnitude of the first three terms on the right hand (RHS) of Eq. (6) is u'^2/δ_t or less. Here,
131 δ_t is the mean flame brush thickness.

132 To estimate the order of magnitude of the last term, let us, first, similarly to Bilger,²⁸ assume
133 that $|\nabla \cdot \mathbf{u}'_p|$ is on the order of $\Theta = (\sigma - 1)\tau_f^{-1}$. This assumption is in line with recent DNS
134 and experimental data, which indicate that combustion is mainly localized to inherently
135 laminar flamelets even at sufficiently high Ka , as reviewed elsewhere.^{34,35} DNS data reported
136 in Sect. IV support this assumption. It is also worth remembering that eventual decrease in

dilatation due to local flame broadening by small-scale turbulent eddies may be counterbalanced by (i) an increase in the dilatation magnitude due to straining of the local flame by larger turbulent eddies³⁶ and (ii) differential diffusion effects,³⁷ which are discussed in detail elsewhere.³⁸

Second, to estimate the magnitude of the fourth term, let us also note that the correlation between solenoidal velocity fluctuations \mathbf{u}'_s and dilatation $\nabla \cdot \mathbf{u}'_p$ does not vanish, because the vorticity transport equation involves a dilatation term.¹⁶⁻¹⁹ This consideration will also be supported in Sect. IV.

Thus, the fourth term on the RHS of Eq. (6) is expected to be on the order of $u'\theta = u'(\sigma - 1)\tau_f^{-1}$ bearing in mind that \mathbf{u}'_s and \mathbf{u}' are of the same order when the thermal expansion effects become relatively weak (close to the boundary we seek for). Therefore, the considered term, which involves potential velocity fluctuations, should play an important role unless the dilatation θ is much smaller than u'/δ_t . Contrary to Eq. (2), this newly introduced criterion compares θ with the large-scale gradient of the rms turbulent velocity in the mean flame brush, rather than with the small-scale velocity gradient in Kolmogorov eddies. As the former gradient is significantly smaller, the newly introduced criterion implies importance of thermal expansion effects in a wider domain of flame characteristics.

According to the new criterion, thermal expansion effects are of minor importance if the Damköhler number $Da = \tau_t/\tau_f$ is less than a critical value of

$$Da_{cr}^{-1} = (\sigma - 1) \frac{\delta_t}{L}, \quad (7)$$

where $\tau_t = L/u'$ is an integral time scale of turbulence.

The same criterion can be obtained in a different way. Let us consider the following well-known Reynolds-averaged transport equation^{16-19,26,35}

$$\frac{\partial c}{\partial t} + u_k \frac{\partial c}{\partial x_k} = \frac{1}{\rho} \frac{\partial q_{c,k}}{\partial x_k} + \frac{1}{\rho} \dot{\omega}_c \quad (8)$$

for a combustion progress variable c , which characterizes mixture state in a flame and varies from zero in unburnt reactants to unity in the equilibrium adiabatic combustion products. Here, $q_{c,k}$ is k -th component of molecular flux \mathbf{q}_c of c and $\dot{\omega}_c$ is the mass rate of product creation. The convection term, i.e., the second term on the LHS of Eq. (8), reads

$$u_k \frac{\partial c}{\partial x_k} = \frac{\partial u_k c}{\partial x_k} - c \frac{\partial u_k}{\partial x_k} = \frac{\partial u_{s,k} c}{\partial x_k} + \frac{\partial u_{p,k} c}{\partial x_k} - c \frac{\partial u_{p,k}}{\partial x_k}. \quad (9)$$

For the reasons presented above, within the mean flame brush, the order of magnitude of the first two terms on the RHS of Eq. (9) is u'/δ_t or less, whereas the order of magnitude of the third term is Θ . Thus, we arrive at Eq. (7) again.

In Eq. (7), the thickness δ_t is unknown *a priori*. Various experimental³⁹⁻⁴² and DNS^{34,43-45} data show that $\delta_t/L > 1$. Therefore, Da_{cr} should be less than $(\sigma - 1)^{-1} = O(10^{-1})$. Moreover, DNS data^{43,44} indicate that mean thickness of a fully-developed turbulent premixed flame, i.e., a turbulent premixed flame propagating at a constant speed and having a constant thickness, scales as $\delta_{t,\infty}/L \propto (u'/S_L)^{1/3}$ in moderately intense ($u'/S_L \leq 10$, $Da > 0.2$) turbulence, whereas a subsequent DNS study³⁴ has yielded $\delta_{t,\infty}/L \propto Da^{-1/2}$ at $Da < 0.1$. Here, the subscript ∞ refers to the fully-developed flame. Let us invoke the latter scaling for δ_t/L , because Eq. (7) implies that a small $Da < O(10^{-1})$ is required for the thermal expansion effects to be of minor importance in turbulent flames. We arrive at

$$Da_{cr} = (\sigma - 1)^{-2} \quad (10)$$

by disregarding numerical factors of unity order.

In the following the thickness $\delta_t = (T_b - T_u)/\max|\nabla T|$ will be extracted from the DNS data.

182 B. Favre-average framework

183 In the combustion literature, Favre averaging is often used to reduce the number of unclosed
184 terms in the Favre-averaged transport equations when compared to the Reynolds-averaged
185 ones. Therefore, it is worth comparing contributions of potential and solenoidal velocities to
186 the Favre-averaged second moments $\overline{\rho u_i'' u_k''}$. Here, $u_i'' \equiv u_i - \tilde{u}_i$ and $\tilde{u}_i \equiv \overline{\rho u_i} / \bar{\rho}$. However,
187 defining Favre-averaged fluctuating solenoidal and potential velocity fields is not trivial.
188 Indeed, because

$$\begin{aligned} 189 \quad u_i'' &= u_i - \tilde{u}_i = \bar{u}_i + u_i' - \tilde{u}_i = \bar{u}_i + u_i' - \frac{\overline{\rho u_i}}{\bar{\rho}} \\ 190 \quad &= \bar{u}_i + u_i' - \frac{\overline{\rho u_i}}{\bar{\rho}} - \frac{\overline{\rho u_i'}}{\bar{\rho}} = u_i' - \frac{\overline{\rho u_i'}}{\bar{\rho}} = u_i' - \tilde{u}_i', \end{aligned} \quad (11)$$

191 the fields $\mathbf{u}'(\mathbf{x}, t)$ and $\mathbf{u}''(\mathbf{x}, t)$ cannot be divergence-free (or irrotational) simultaneously.
192 Since $\mathbf{u}'(\mathbf{x}, t)$ directly characterizes the fluctuating velocity field, whereas $\mathbf{u}''(\mathbf{x}, t)$ is also
193 affected by the density, HHD should be applied to $\mathbf{u}'(\mathbf{x}, t)$, followed by computation of the
194 velocities \mathbf{u}_s'' and \mathbf{u}_p'' using Eq. (11), i.e.,

$$195 \quad u_{s,i}'' \equiv u_{s,i}' - \tilde{u}_{s,i}', \quad u_{p,i}'' \equiv u_{p,i}' - \tilde{u}_{p,i}'. \quad (12)$$

196 Subsequently, contributions of the solenoidal and potential velocity fields to the Favre-
197 averaged Reynolds stress term can be evaluated as follows

$$198 \quad \frac{\partial}{\partial x_k} \overline{\rho u_i'' u_k''} = \underbrace{\frac{\partial}{\partial x_k} \overline{\rho u_{s,i}'' u_{s,k}''}}_{T_1} + \underbrace{\frac{\partial}{\partial x_k} \overline{\rho u_{p,i}'' u_{p,k}''}}_{T_2} + \underbrace{\frac{\partial}{\partial x_k} \overline{\rho u_{p,i}'' u_{s,k}''} + \frac{\partial}{\partial x_k} \overline{\rho u_{s,i}'' u_{p,k}''}}_{T_3}, \quad (13)$$

199 where $u_{s,i}''$ and $u_{p,i}''$ are defined by Eq. (12). Various terms in Eqs. (6) and (13) will be
200 compared in Sect. IV by analyzing DNS data obtained from two flames characterized by
201 different Ka .

202 Note that the Favre-averaged convection term is also affected by fluctuating solenoidal and
 203 potential velocities. Indeed, substitution of $\tilde{u}_i = \overline{u_i} + \tilde{u}'_i = \bar{u}_i + \tilde{u}'_i$ into a product of $\tilde{u}_i \tilde{u}_k$,
 204 followed by application of HHD to the fields $\bar{\mathbf{u}}(\mathbf{x}, t)$ and $\mathbf{u}'(\mathbf{x}, t)$ results in a sum of 16 terms.
 205 In the statistically 1D and planar case, $\bar{u}_{p,1} = \bar{u}_1$, $\bar{u}_{s,1} = 0$, and

$$\begin{aligned} \frac{\partial}{\partial x_1} (\bar{\rho} \tilde{u}_1^2) = & \underbrace{\frac{\partial}{\partial x_1} (\bar{\rho} \tilde{u}_{s,1} \tilde{u}_{s,1})}_{\tilde{T}_1} + 2 \underbrace{\frac{\partial}{\partial x_1} (\bar{\rho} \tilde{u}_{s,1} \bar{u}_1)}_{\tilde{T}_2} + 2 \underbrace{\frac{\partial}{\partial x_1} (\bar{\rho} \tilde{u}_{s,1} \tilde{u}_{p,1})}_{\tilde{T}_3} \\ & + \underbrace{\frac{\partial}{\partial x_1} (\bar{\rho} \bar{u}_1^2)}_{\tilde{T}_4} + 2 \underbrace{\frac{\partial}{\partial x_1} (\bar{\rho} \tilde{u}_{p,1} \bar{u}_1)}_{\tilde{T}_5} + \underbrace{\frac{\partial}{\partial x_1} (\bar{\rho} \tilde{u}_{p,1} \tilde{u}_{p,1})}_{\tilde{T}_6}. \end{aligned} \quad (14)$$

208 III. NUMERICAL SIMULATIONS

209 A. DNS conditions

210 As the DNS attributes and data were reported earlier,^{11,15,46-48} only a brief description is
 211 given below, with more details being reported in Appendix A. Unconfined statistically 1D
 212 and planar, lean (the equivalence ratio $\Phi=0.7$) H_2 -air turbulent flames were investigated by (i)
 213 adopting a detailed (9 species, 23 reversible reactions) chemical mechanism⁴⁹ with the
 214 mixture-averaged transport model and (ii) numerically solving unsteady three-dimensional
 215 governing equations, written in compressible form. Note that while differential diffusion
 216 effects are well known to be highly pronounced in very lean H_2 -air flames and to significantly
 217 increase turbulent burning velocity, as reviewed elsewhere,³⁸ differential diffusion was
 218 shown^{50,51} to weakly affect a mean bulk burning rate at $\Phi=0.7$. For this reason, the equivalence
 219 ratio was set equal to 0.7 in the present study.

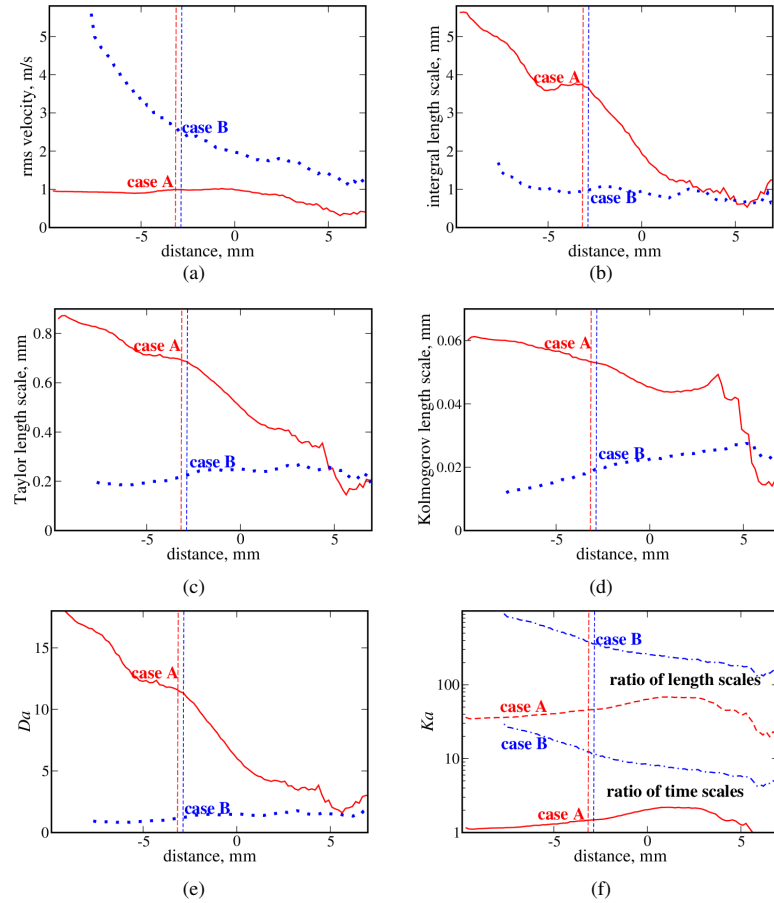


FIG. 1. Axial variations of turbulent flame characteristics conditioned to unburned mixture in flames A (red lines) and B (blue lines). Vertical dotted-dashed lines show the flame-brush leading edge, i.e., planes characterized by $\bar{c}(\xi) = 0.05$. (a) rms turbulent velocity u' , (b) integral length scale L_{KE} , (c) Taylor microscale λ , (d) Kolmogorov length scale η_K , (e) Damköhler number, (f) Karlovitz number $Ka = \tau_f/\tau_K$ and $(\delta_L/\eta_K)^2$.

Two cases A and B, characterized by two different values of the inlet rms velocity, with all other things being equal, were studied. Variations of the major turbulence characteristics along the x -axis in these two cases are shown in Fig. 1. Here, the distance ξ is counted from a transverse plane characterized by $\langle c \rangle(x, t) = 0.5$ at each instant, i.e., $\langle c \rangle(\xi, t) = 0.5$; the

225 combustion progress variable c is defined using fuel mass fraction; all reported quantities
 226 $\langle \cdot | c < 0.02 \rangle$ are conditioned to unburned mixture, i.e., to $c(\mathbf{x}, t) < 0.02$, and, subsequently,
 227 are transverse and time-averaged; $u' = \sqrt{2\langle u'_k u'_k | c < 0.02 \rangle / 3}$; $L_{k\varepsilon} =$
 228 $\langle 0.5 u'_k u'_k | c < 0.02 \rangle^{3/2} / \langle \varepsilon | c < 0.02 \rangle$; $Da = L_{k\varepsilon} S_L / (u' \delta_L)$; $Ka = \tau_f / \tau_K$, with a ratio of
 229 $(\delta_L / \eta_K)^2$ being also plotted in Fig. 1f; $\tau_K = (\nu_u / \langle \varepsilon | c < 0.02 \rangle)^{1/2}$ and $\eta_K =$
 230 $(\nu_u^3 / \langle \varepsilon | c < 0.02 \rangle)^{1/4}$; $\lambda = 15 \nu_u u'^2 / \langle \varepsilon | c < 0.02 \rangle$ is Taylor microscale; and the local
 231 dissipation rate $\varepsilon = 2 \nu_u S_{jk} S_{jk}$. A slow decrease in η_K with the streamwise distance near the
 232 leading edge of flame A (see red solid line in Fig. 1d) is attributed to the influence of
 233 combustion-induced thermal expansion on turbulence upstream of the flame, as will be
 234 discussed later (see Fig. 7a in Sect. IV).

235

Table I. Relevant parameters characterizing the DNS cases.									
	u'_0 / S_L	L_T / δ_L	Re_T	u' / S_L	$L_{k\varepsilon} / \delta_L$	Da	Ka	$(\delta_L / \eta_K)^2$	Da_{cr}
A	0.7	14	227	0.7	10.3	11	1.5	46	0.11
B	5.0	14	1623	1.9	2.7	1.2	12	385	0.03

236 Major characteristics of the injected turbulence and major turbulent flame characteristics
 237 evaluated at the leading edges of the two flame brushes are reported in Table I. Here, u'_0 is the
 238 rms velocity in the injected flow; L_T is the most energetic length scale of the Passot-Pouquet
 239 spectrum;⁵² $Re_T = u'_0 L_T / \nu_u$; the quantities u' , $L_{k\varepsilon}$, Da , and Ka have been sampled at $\overline{c(\xi)} =$
 240 0.05; $S_L = 1.36$ m/s, $\delta_L = 0.36$ mm, $\sigma = 6.7$, and, hence, $Ka_{cr}^B = 5.7$ have been computed
 241 under the simulation conditions (atmospheric pressure and $T_u = 300$ K); Da_{cr} has been
 242 calculated using Eq. (7) and the DNS data on $\delta_t = (T_b - T_u) / \max|\nabla \bar{T}|$, whereas Eq. (10)
 243 yields $Da_{cr} = 0.03$ for both flames. In case B, Eqs. (7) and (10) yield close results. In case
 244 A, the Damköhler number is significantly higher; consequently, scaling of $\delta_t \propto \delta_L \sqrt{Re_T}$ does
 245 not hold and results yielded by Eqs. (7) and (10) are different. Note also that $(\delta_L / \eta_K)^2$ is

246 much larger than $Ka = \tau_f / \tau_K$, because $\delta_L = (T_b - T_u) / \max|\nabla T| \gg \nu_u / S_L$ in the studied
247 complex-chemistry case.

248 The criteria introduced in Sect. II, both Eq. (7) and Eq. (10), imply that combustion-induced
249 thermal expansion can substantially affect the large-scale turbulence characteristics in both
250 flames A and B. On the contrary, Eq. (2) suggests that the influence of the thermal expansion
251 on the small-scale turbulence characteristics can be of importance in flame A only, whereas
252 $Ka > Ka_{cr}^B$ in case B.

253 When processing the DNS data, transverse-averaged quantities $\langle \cdot \rangle(\xi, t)$ were sampled first,
254 followed by time-averaging of them. Time and transverse-averaged quantities are designated
255 with overbar, e.g., $\bar{c}(\xi) \equiv \overline{\langle c \rangle(\xi, t)}$.

256 B. Helmholtz-Hodge decomposition

257 The fluctuating velocity $\mathbf{u}'(\mathbf{x}, t)$ was decomposed into solenoidal and potential components
258 $\mathbf{u}'_s(\mathbf{x}, t)$ and $\mathbf{u}'_p(\mathbf{x}, t)$ by using two methods: (i) conventional³³ HHD and (ii) natural^{53,54}
259 decompositions. To do so, algorithms that were applied earlier by the present authors to
260 velocity fields obtained from weakly turbulent single-step chemistry flames^{55,56} and from
261 flames¹⁵ A and B were adopted. The reader interested in a detailed discussion of these
262 algorithms is referred to the latter paper.¹⁵ Since the earlier results yielded by the two
263 decompositions were hardly distinguishable within flame brushes,⁵⁵ we will report results
264 obtained using the former method only.

265 The fields $\mathbf{u}''_s(\mathbf{x}, t)$ and $\mathbf{u}''_p(\mathbf{x}, t)$ were computed using Eq. (12). Note that $\nabla \cdot \mathbf{u}''_s \neq 0$ and
266 $\nabla \times \mathbf{u}''_p \neq 0$.

IV. NUMERICAL RESULTS AND DISCUSSION

To obtain Eqs. (7) and (10) in Sect. II, two assumptions were invoked: (i) correlation between solenoidal velocity fluctuations and dilatation did not vanish and (ii) the order of magnitude of local dilatation in turbulent premixed flames could be estimated using the laminar-flame value Θ . These assumptions are validated in Figs. 2 and 3, respectively.

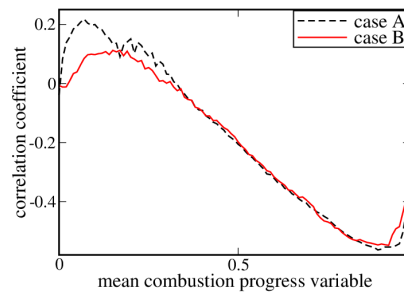


FIG. 2. Correlation coefficient $\overline{u'_{s,1} \nabla \cdot \mathbf{u}'_p} / [\overline{u'^2_{s,1}} (\nabla \cdot \mathbf{u}'_p)^2]^{1/2}$ vs. mean combustion progress \bar{c} .

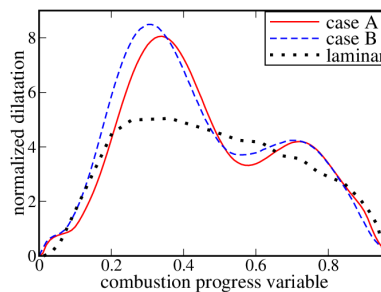


FIG. 3. Conditioned dilatation $\langle \nabla \cdot \mathbf{u} | c \rangle$ sampled from the entire computational domain in case A or B, as well as dependence of $\nabla \cdot \mathbf{u}$ on c in the counterpart laminar flame.

More specifically, Fig. 3 shows that the conditioned dilatation $\langle \nabla \cdot \mathbf{u} | c \rangle$ is indeed on the order of $\nabla \cdot \mathbf{u}(c)$ in the laminar flame, while the former can be larger than the latter. A similar quantitative difference was reported in earlier DNS studies.^{36,37} Such a difference can be

280 controlled by three physical mechanisms: (i) local flame thinning due to turbulent stretch rates,
 281 (ii) local flame broadening due to small-scale turbulent mixing, and (iii) differential diffusion
 282 effects if molecular transport coefficients for fuel, oxidant, and heat are substantially different.
 283 Mechanisms (i) and (ii) always compete and can either decrease or increase the local flame
 284 thickness depending on conditions.⁵⁷ Accordingly, the local dilatation is either increased or
 285 decreased, respectively. Differential diffusion effects can change not only the local flame
 286 thickness but also the local normal velocity jump at the flame. While for the considered
 287 mixture, mean bulk burning rate was shown to be weakly affected by differential diffusion,
 288 variations in the local flame characteristics were also documented.^{50,51} Further discussion of
 289 Fig. 3 is beyond the scope of the present work, and differences between the turbulent $\langle \nabla \cdot \mathbf{u} | c \rangle$,
 290 see solid and dashed lines, and the laminar $\nabla \cdot \mathbf{u}(c)$, see dotted line, could be addressed in a
 291 future study.

292 Figure 4 shows variations of all terms in Eq. (6) within mean flame brushes. Note that the
 293 almost perfect agreement between the LHS and RHS of this equation in both cases, cf. black
 294 solid and brown dotted lines, verifies conservation in the simulations. Contrary to the criterion
 295 given by Eq. (2), but in line with the newly introduced criterion given by Eq. (7), thermal
 296 expansion effects are well pronounced not only in flame A, but also in flame B. More
 297 specifically, the magnitude of the last term (T_4), which contains dilatation and, hence, arises
 298 due to thermal expansion, is comparable with or larger than the magnitude of the purely
 299 solenoidal term T_1 . Furthermore, at $\bar{c} > 0.5$, the former term dominates within both flames,
 300 i.e., $|T_4|$ is much larger than $|T_1 + T_2 + T_3|$. These DNS data clearly show importance of
 301 thermal expansion effects under conditions of the present study, thus, supporting the analysis
 302 in Sect. II. Note that (i) $T_4 < 0$ at $\bar{c} > 0.5$ because dilatation reduces vorticity in flames,¹⁶⁻¹⁹
 303 i.e., correlation between solenoidal velocity fluctuations and dilatation is predominantly

negative (see Fig. 2); but (ii) the RHS of Eq. (6) is positive because it includes T_4 with a minus sign.

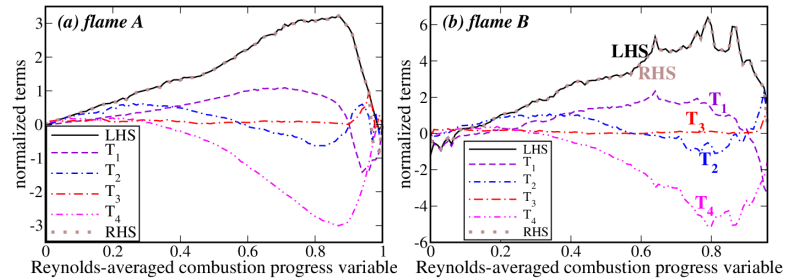


FIG. 4. Various terms in Eq. (6), normalized using S_L and δ_L , in flames (a) A and (b) B.

Importance of thermal expansion effects is also shown in Fig. 5, which reports various terms in Eq. (13) for the two statistically one-dimensional planar flames (note almost perfect matching between the LHS and RHS again). Although the magnitude of the solenoidal term T_1 is larger than the magnitudes of other terms at $\bar{c} > 0.5$ in both flames and at $\bar{c} < 0.2$ in flame B, term T_3 , which involves both solenoidal and potential velocities, also plays an important role. Even the potential term T_2 is not negligible.

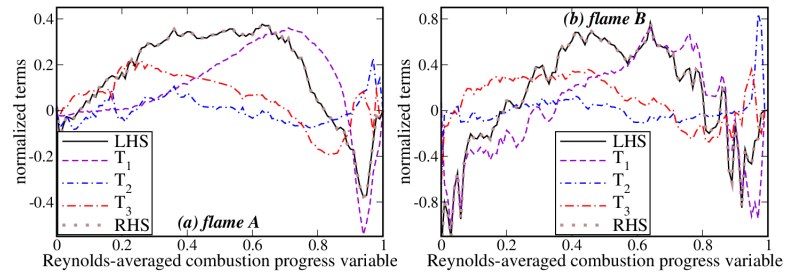


FIG. 5. Various terms in Eq. (13), normalized using ρ_u , S_L , and δ_L , in flames (a) A and (b) B.

At the same time, comparison of Figs. 4 and 5 indicates that thermal expansion effects are less pronounced within the Favre-averaging framework, i.e., the dilatation term (T_4)

dominates at $\bar{c} > 0.5$ on the RHS of Eq. (6), whereas the solenoidal term (T_1) is the most important term on the RHS of Eq. (13) in the largest parts of the two flame brushes. However, this result does not mean that the use of Favre-averaged velocities is favorable in solving the problem of modeling turbulence in flames. The fact that the solenoidal term is the largest term on the RHS of Eq. (13) at $\bar{c} > 0.5$ does not prove that models developed for solenoidal incompressible turbulent flows hold for the solenoidal term on the RHS of Eq. (13) in flames. Rather, combustion-induced thermal expansion can substantially affect not only potential velocity fluctuations, but also solenoidal turbulence even at high Ka . Two examples follow.

First, Fig. 3 and a large magnitude of term T_4 on the RHS of Eq. (6) (see Fig. 4) show a well-pronounced negative (at $\bar{c} > 0.4$) correlation between dilatation and solenoidal velocity fluctuations, thus implying a substantial influence of thermal expansion on the solenoidal velocity field in the studied flames.

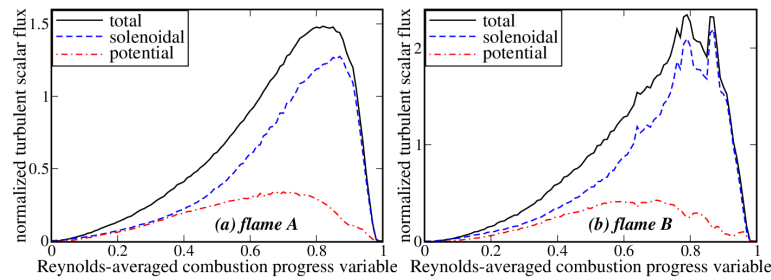


FIG. 6. Axial turbulent scalar flux normalized using ρ_u and S_L in flames (a) A and (b) B.

Second, Fig. 6 shows that not only the total turbulent scalar flux $\overline{\rho u'' c''}$, but also its solenoidal and potential components are counter-gradient ($d\bar{c}/dx > 0$ in the studied flames). The counter-gradient behavior of $\overline{\rho u_s'' c''}$ indicates a substantial influence of thermal expansion on the solenoidal velocity in the considered flames. This influence is attributed to vorticity that is generated by baroclinic torque. As discussed in detail elsewhere,^{6,8} such a

337 vorticity acts to push the leading and trailing segments of the instantaneous flame inside the
 338 mean flame brush. Thus, for a flame propagating from right to left, fluctuations in the local
 339 u_s , caused by baroclinic torque, are positive and negative at $\bar{c} \ll 1$ and $1 - \bar{c} \ll 1$,
 340 respectively. Fluctuations in the local c , caused by appearance of the instantaneous flame, are
 341 also positive and negative in these zones, respectively. Therefore, u'_s correlates positively with
 342 c' . It is worth noting that the obtained counter-gradient behavior of the flux $\overline{\rho u'' c''}$ does not
 343 contradict the well-known Bray number criterion,^{26,27} because $u'/S_L < \sigma - 1$ even in case B.
 344 As evidenced by the above analysis, there is substantial influence of combustion-induced
 345 thermal expansion not only on the total and potential velocity fluctuations, but also on the
 346 solenoidal velocity fluctuations at $Ka = \tau_f/\tau_K$ as large as 12 and $(\delta_L/\eta_K)^2$ about 400.

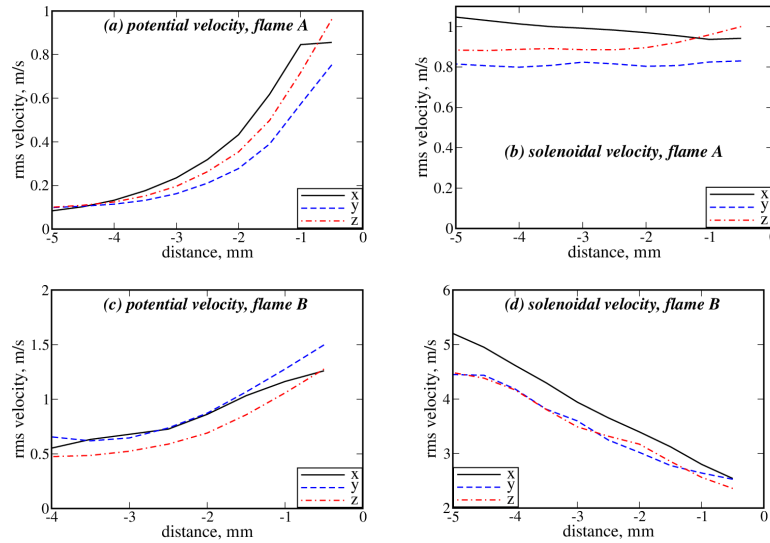


FIG. 7. Variations of (a), (c) potential and (b), (d) solenoidal rms velocities $(\overline{u'^2})^{1/2}$ and $(\overline{u'^2})^{1/2}$, respectively, upstream of flames (a)-(b) A and (c)-(d) B. Zero distance corresponds to $\langle c \rangle(x, t) = 0.01$.

347

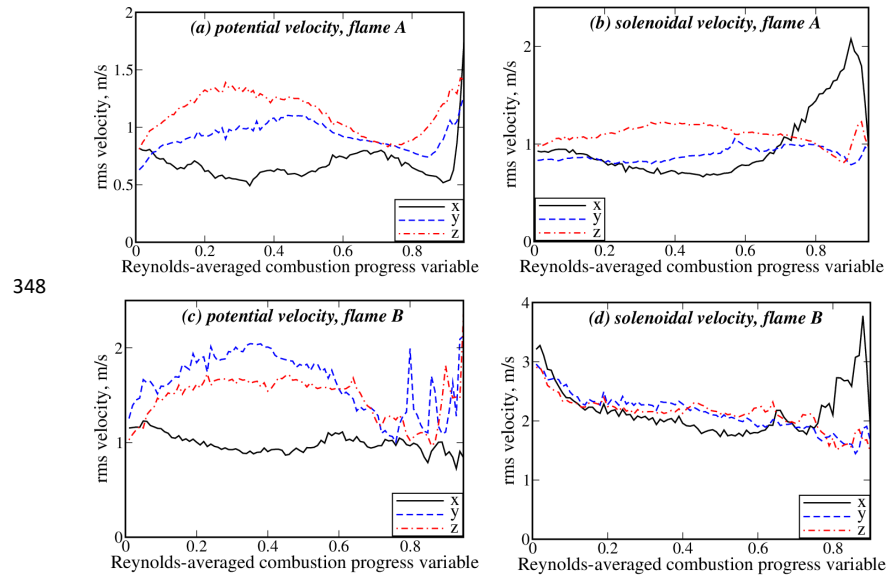


FIG. 8. Variations of (a), (c) potential and (b), (d) solenoidal rms velocities conditioned to unburned mixture, i.e., $\langle u_{i,p}^2 | c(\mathbf{x}, t) < 0.01 \rangle^{1/2}$ and $\langle u_{i,s}^2 | c(\mathbf{x}, t) < 0.01 \rangle^{1/2}$, respectively, within flames (a)-(b) A and (c)-(d) B.

Further insights into the influence of combustion-induced thermal expansion on turbulence in flames can be obtained from Figs. 7 and 8. In particular, Figs. 7a and 7c show that the rms magnitude $\langle u_{i,p}^2 \rangle^{1/2}$ of the potential velocity fluctuations increases upstream of the flame brush as the flow approaches the flame leading edge $\langle c \rangle(x, t) = 0.01$. This effect is attributed to generation of potential velocity fluctuations by combustion-induced pressure perturbations that propagate upstream of the flame. A similar physical mechanism is well known to cause the hydrodynamic instability of laminar premixed flames.^{58,59} On the contrary, the solenoidal $\langle u_{i,s}^2 \rangle^{1/2}$ decreases with distance from the inlet due to turbulence decay, which is much more pronounced in the highly turbulent case B. As a result, the potential and solenoidal rms

358 velocities are comparable in the region close to the flame leading edge, cf. rightmost points
359 on curves in Figs. 7a and 7b for case A, and Figs. 7c and 7d for case B.

360 Last, Fig. 8 shows that rms values of potential and solenoidal velocity fluctuations,
361 conditioned to unburned gas are comparable with one another within A or B-flame brush.

362 V. TURBULENCE-IN-PREMIXED-FLAME DIAGRAM

363 The goal of this section is to discuss different criteria of importance of thermal expansion
364 effects in premixed flames and to present such criteria in a regime diagram. While this diagram
365 seems similar to the classical premixed-turbulent-combustion regime-diagrams,⁶⁰⁻⁶² there is
366 an important difference: the classical diagrams address the influence of turbulence on a
367 premixed flame, whereas the present diagram considers the influence of a premixed flame on
368 turbulence.

369 First, let us compare the two criteria given by Eqs. (2) and (10). Using the well-known
370 scaling of $Da^2 Ka^2 \propto Re_t = u'L/\nu$, where constants of unity order are omitted for brevity,
371 the critical number Da_{cr} could be substituted with $\sqrt{Re_t}/Ka_{cr}$. Accordingly, Eq. (10) reads

$$372 \quad Ka_{cr} = (\sigma - 1)^2 \sqrt{Re_t} = Ka_{cr}^B (\sigma - 1) \sqrt{Re_t} \gg Ka_{cr}^B. \quad (15)$$

373 Alternatively, Eq. (2) can be rewritten as follows

$$374 \quad Da_{cr}^B = \sqrt{Re_t} (\sigma - 1)^{-1} = (\sigma - 1) \sqrt{Re_t} Da_{cr} \gg Da_{cr}. \quad (16)$$

375 Thus, the newly introduced criterion substantially extends the domain of the influence of
376 combustion-induced thermal expansion on turbulence in premixed flames to a higher
377 Karlovitz number and a lower Damköhler number. The DNS data analyzed in Sect. IV and,
378 in particular, Figs. 4, 5, 7, and 8 are consistent with this extension.

379 Second, as noted in Sect. I, O'Brien et al.²⁸ have theorized that backscatter can arise from
 380 smaller scales, associated with injection of kinetic energy due to combustion, to larger scales
 381 whose lifetime τ_m is shorter than or equal to the laminar flame time scale τ_f . In the inertial
 382 range²⁹ of Kolmogorov turbulence, a constraint of $\tau_m \leq \tau_f$ reads $(l_m^2/\varepsilon)^{1/3} \leq \tau_f$ or

$$383 \quad l_m \leq (\bar{\varepsilon}\tau_f^3)^{1/2} = S_L^{-3/2}\delta_L^{3/2}(\nu_u/\tau_K^2)^{1/2} = \delta_L Ka\Gamma^{-1/2}, \quad (17)$$

384 with the length scale $(\bar{\varepsilon}\tau_f^3)^{1/2}$ being earlier introduced by Corrsin.⁶³ Here, the number $\Gamma \equiv$
 385 $S_L\delta_L/\nu_u$, known as “flame Reynolds number”, is larger than unity and can be as large as 50
 386 in lean hydrogen-air mixtures under room conditions.⁶⁴ If the energy flux due to combustion
 387 is localized to scales on the order of δ_L ,⁶⁵⁻⁶⁷ the scale l_m should be larger than δ_L . Therefore,
 388 Eq. (17) implies that backscatter could arise if $Ka\Gamma^{-1/2} > 1$ or

$$389 \quad Ka > \Gamma^{1/2}. \quad (18)$$

390 If $Ka < \Gamma^{1/2}$, even the smallest turbulent eddies evolve slowly, such that combustion-induced
 391 local velocity perturbations are associated with rapid distortion within the flame, and “any
 392 cascade interaction through convective transport between small and large scales is relegated
 393 to the far wake of the burnt gases.”³²

394 Equation (17) is a necessary condition for existence of a spectral interval where backscatter
 395 can be induced by combustion. However, to cause backscatter, combustion should be
 396 sufficiently strong. By extending Bilgers' arguments,²⁸ let us hypothesize that backscatter may
 397 arise if the dilatation Θ is larger than the magnitude of turbulence-induced velocity gradient
 398 $(\delta_L^2/\varepsilon)^{-1/3}$ at the scale $l = \delta_L$, associated with the energy injection due to combustion. Here,
 399 this length scale is assumed to belong to the inertial range of turbulence spectrum, which
 400 seems to be plausible if $Ka > Ka_{cr}^B > 1$ (especially for lean hydrogen-air mixtures, where

401 $\delta_L/\eta_K \gg Ka^{1/2}$ under room conditions). Therefore, backscatter may arise in the inertial
402 range if

$$403 \quad \Theta(\delta_L^2/\bar{\epsilon})^{1/3} = (\sigma - 1)S_L\delta_L^{-1/3}(\tau_K^2/\nu_u)^{1/3} = (\sigma - 1)Ka^{-2/3}(S_L\delta_L/\nu_u)^{1/3} > 1 \quad (19)$$

404 or

$$405 \quad Ka < Ka_{cr}^* = (\sigma - 1)^{3/2}\Gamma^{1/2} = (\sigma - 1)^{1/2}\Gamma^{1/2}Ka_{cr}^B. \quad (20)$$

406 Since $Ka_{cr}^* > Ka_{cr}^B$ and $\Gamma^{1/2} < Ka_{cr}^B$ for most fuels (or $\Gamma^{1/2} \cong Ka_{cr}^B$ in lean hydrogen-air
407 mixtures), Eqs. (18) and (20) are consistent with one another. Under conditions of $\Gamma^{1/2} <$
408 $Ka < Ka_{cr}^*$, both $\Gamma^{1/2} < Ka < Ka_{cr}^B$ and $\Gamma^{1/2} < Ka_{cr}^B < Ka$ are possible, i.e., Eq. (2) may
409 or may not hold. Thus, backscatter may arise even if the smallest-scale turbulent eddies are
410 weakly affected by combustion-induced thermal expansion.

411 For the present flame B, $Ka = 12$ (see Table I) is larger than $Ka_{cr}^B = 5.7$, but is smaller
412 than $Ka_{cr}^* = 75$. Accordingly, substantial influence of combustion-induced thermal
413 expansion on turbulent eddies from the inertial range is expected. Indeed, two-point second-
414 order structure functions for the potential velocity field, which (i) were sampled from flame
415 B, (ii) were conditioned to unburnt mixture, and (iii) were reported in a recent paper,¹⁵ do
416 show such an influence even at small distances r between two points where velocity is picked.
417 In flame A characterized by $Ka < Ka_{cr}^B$, the effect is observed even at very small r , cf. Figs.
418 4b and 4e or 4c and 4f in the cited paper, where flames A and B are labeled with letters W and
419 H, respectively.

420 Using a scaling of $Da^2Ka^2 \propto Re_t$, Eq. (20) reads

$$421 \quad Da > Da_{cr}^* = \sqrt{Re_t}(\sigma - 1)^{-3/4}\Gamma^{-1/4} = \sqrt{Re_t}(\sigma - 1)^{5/4}\Gamma^{-1/4}Da_{cr}. \quad (21)$$

Therefore, $Da_{cr}^* > Da_{cr}$ if $Re_t > (\sigma - 1)^{-5/2} \Gamma^{1/2}$, which holds in a turbulent flow, where $Re_t \gg 1$. Thus, when compared to Eq. (20), which allows for backscatter in the inertial range, the newly introduced criterion given by Eq. (10) substantially extends the domain of the influence of combustion-induced thermal expansion on turbulence in premixed flames to a lower Damköhler number.

In addition to the three criteria given by Eqs. (2), (10), and (20), one more criterion is worth mentioning. Hydrodynamic instability of laminar premixed flames^{58,59} stems from velocity perturbations upstream of the flame, caused by combustion-induced pressure waves. Thus, the instability is an example of the discussed thermal expansion effects. However, as shown elsewhere,^{38,68-70} the instability plays a minor role in premixed turbulent combustion if Ka is of unity order or larger. Therefore, the instability cannot change the three criteria given by Eqs. (2), (10), and (20).

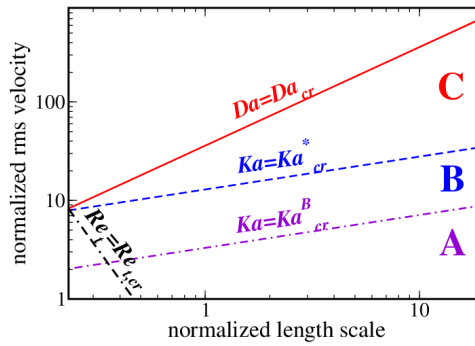


FIG. 9. Turbulence-in-premixed-flame diagram $\{L/\delta_L, u'/S_L\}$ sketched using Eq. (2) (violet dotted-dashed line), Eq. (10) (red solid line), Eq. (20) (blue dashed line), and Eq. (22) (black double-dashed-dotted line). $\sigma = 7$, $\Gamma = 10$, and $u'/S_L = Ka^{2/3}(L/\delta_L)^{1/3}$. A: region of the influence of thermal expansion on small-scale turbulence. B: active cascade region. C: region of the influence of thermal expansion on large-scale turbulence.

The three criteria given by Eqs. (2), (10), and (20) are plotted in violet dotted-dashed, red solid, and blue dashed lines, respectively, in Fig. 9. To do so, values of $\sigma = 7$ and $\Gamma = 10$,

437 associated with near-stoichiometric methane-air mixtures under room conditions, were set and
 438 the following simplified relation $u'/S_L = Ka^{2/3}(L/\delta_L)^{1/3}$ was invoked. Since Eq. (10) was
 439 obtained using Eq. (7) and the following scaling $\delta_{t,\infty}/L \propto Re_t^{1/2}$, extrapolation of Eq. (10) to
 440 low length scale ratios L/δ_L is limited by a constraint of $\delta_{t,\infty} > \delta_L$ or

$$441 \quad Re_t > Re_{t,cr} = \left(\frac{\delta_L}{L}\right)^2. \quad (22)$$

442 In Fig. 9, this constraint is plotted in black double-dashed-dotted line.

443 In the domain bounded by Eqs. (10) and (20), combustion-induced thermal expansion can
 444 affect large-scale turbulence characteristics, as discussed in Sects. III and V. In a band
 445 bounded by Eqs. (2) and (20), the combustion-induced thermal expansion can also cause
 446 backscatter in the inertial range of turbulence spectrum. Following O'Brien et al.,³² this layer
 447 is labeled “active cascade”. Note that Eq. (18) holds for the selected values of $\sigma = 7$ and $\Gamma =$
 448 10. Finally, below the violet dotted-dashed line yielded by Eq. (2), the combustion-induced
 449 thermal expansion can also affect the smallest turbulent eddies.

450 VI. CONCLUSIONS

451 A new criterion was introduced for assessing importance of turbulence modulations due to
 452 combustion-induced thermal expansion in premixed flames. The criterion highlights a ratio of
 453 dilatation in the laminar flame to the large-scale gradient of rms turbulent velocity across the
 454 turbulent flame brush. When compared to the well-known Bilger's criterion,²⁸ the developed
 455 criterion substantially expands domain of conditions associated with importance of thermal
 456 expansion. It is worth stressing, however, that the present study extends Bilger's analysis,²⁸
 457 rather than contradicting it. The point is that Bilger²⁸ addressed the influence of combustion-

458 induced thermal expansion on small-scale turbulence characteristics, whereas the present
459 work allows for large-scale effects.

460 Assumptions invoked to arrive to the newly introduced criterion were validated by
461 analyzing DNS data obtained earlier from two complex-chemistry, lean H₂-air flames
462 propagating in a box. In line with the new criterion, results show significant influence of
463 combustion-induced potential velocity fluctuations on evolution of the second moments of the
464 turbulent velocity field upstream of and within both flame brushes. In particular, the DNS data
465 show that (i) potential and solenoidal rms velocities are comparable in unburnt gas close to
466 the leading edge of flame brush in each case and (ii) potential and solenoidal rms velocities
467 conditioned to unburnt gas are comparable within entire flame brush in each case.

468 Moreover, the DNS data indicate that combustion-induced thermal expansion affects not
469 only total and potential velocities, but also solenoidal velocity. Such effects manifest
470 themselves in a negative correlation between the solenoidal velocity fluctuations and
471 dilatation or in the counter-gradient behavior of the solenoidal scalar flux $\overline{\rho u_s'' c''}$. Therefore,
472 the applicability of constant-density turbulence models to the solenoidal velocity fluctuations
473 in flames may be subjected to scrutiny even at $(\delta_L/\eta_K)^2$ about 400.

474 To summarize results of earlier relevant studies^{10,28,32} and the present one, various regimes
475 of the influence of combustion-induced thermal expansion on turbulence spectrum in
476 premixed flames are outlined in a newly introduced turbulence-in-premixed-flame (TiPF)
477 diagram.

478 Declaration of Competing Interest

479 The authors declare that they have no known competing financial interests or personal
480 relationships that could have appeared to influence the work reported in this paper.

481 **Acknowledgements**

482 V.A.S. gratefully acknowledges support provided by ONERA and by the Ministry of
483 Science and Higher Education of the Russian Federation (Grant agreement of December 8,
484 2020 No. 075-11-2020-023) within the program for the creation and development of the
485 World-Class Research Center "Supersonic" for 2020-2025. A.N.L. gratefully acknowledges
486 the financial support provided by CERC and Chalmers Area of Advance "Transport".
487 F.E.H.P. and H.G.I. were sponsored by King Abdullah University of Science and Technology
488 (KAUST). Computational resources for the DNS calculations were provided by the KAUST
489 Supercomputing Laboratory.

490 **DATA AVAILABILITY**

491 The data that support the findings of this study are available from the corresponding author
492 upon reasonable request.

493 **APPENDIX A: DNS ATTRIBUTES**

494 Simulations were performed in a rectangular domain of size of $20 \times 10 \times 10 \text{ mm}^3$ using a
495 uniform Cartesian mesh of $512 \times 256 \times 256$ cells. The mesh ensured about ten grid points per
496 δ_L , with Kolmogorov length scale being larger than cell size Δx . Unsteady three-dimensional
497 partially differential transport equations were discretized using an eighth-order central
498 difference scheme for internal mesh points, with the order of differentiation being gradually
499 decreased to a one-sided fourth-order scheme near the inlet and outlet boundaries.⁷¹ Time
500 integration was performed adopting an explicit fourth-order Runge-Kutta scheme.⁷¹

Along the flame propagation direction, inflow and outflow characteristic boundary conditions were set using an improved Navier-Stokes characteristic boundary condition technique.⁷² Other boundary conditions were periodic.

A divergence-free, isotropic, homogeneous turbulent velocity field was generated using a pseudo spectral method⁷³ and adopting the Passot-Pouquet spectrum.⁵² The field was injected through the inlet (left) boundary and decayed along the mean flow direction (x -axis). At $t = 0$, a pre-computed planar laminar flame structure was embedded into the computational domain to initialize turbulent flame propagation from right to left along x -axis. Subsequently, the mean inlet flow velocity was gradually changed to match turbulent flame speed. Results reported in the present paper were sampled at six different instants in each case, i.e., at $t/t_e = 0.57, 0.67, 0.77, 0.86, 0.96$, and 1.05 in case A and at $t/t_e = 4.1, 4.8, 5.5, 6.2, 6.8$, and 7.5 in case B, where, t_e is the eddy turnover time.

References

- ¹B. Karlovitz, D. W. Denniston, and F. E. Wells, "Investigation of turbulent flames," J. Chem. Phys. **19**, 541-547 (1951).
- ²P. A. Libby and K. N. C. Bray, "Countergradient diffusion in premixed turbulent flames," AIAA J. **19**, 205-213 (1981).
- ³C. Dopazo, L. Cifuentes, and N. Chakraborty, "Vorticity budgets in premixed combustng turbulent flows at different Lewis numbers," Phys. Fluids **29**, 045106 (2017).
- ⁴Z. Wang and J. Abraham, "Effects of Karlovitz number on turbulent kinetic energy transport in turbulent lean premixed methane/air flames," Phys. Fluids **29**, 085102 (2017).
- ⁵A. N. Lipatnikov, V. A. Sabelnikov, S. Nishiki, and T. Hasegawa, "Combustion-induced local shear layers within premixed flamelets in weakly turbulent flows," Phys. Fluids **30**, 085101 (2018).
- ⁶A. N. Lipatnikov, V. A. Sabelnikov, S. Nishiki, and T. Hasegawa, "Does flame-generated vorticity increase turbulent burning velocity?" Phys. Fluids **30**, 081702 (2018).
- ⁷P. Brearley, U. Ahmed, N. Chakraborty, and A. N. Lipatnikov, "Statistical behaviours of conditioned two-point second-order structure functions in turbulent premixed flames in different combustion regimes," Phys. Fluids **31**, 115109 (2019).
- ⁸A. N. Lipatnikov, V. A. Sabelnikov, S. Nishiki, and T. Hasegawa, "A direct numerical simulation study of the influence of flame-generated vorticity on reaction-zone-surface area in weakly turbulent premixed combustion," Phys. Fluids **31**, 055101 (2019).
- ⁹A. R. Varma, U. Ahmed, and N. Chakraborty, "Effects of body forces on vorticity and enstrophy evolutions in turbulent premixed flames," Phys. Fluids **33**, 035102 (2021).
- ¹⁰J. F. MacArt and M. E. Mueller, "Damköhler number scaling of active cascade effects in turbulent premixed combustion," Phys. Fluids **33**, 035103 (2021).

This is the author's peer reviewed, accepted manuscript. However, the online version of record will be different from this version once it has been copyedited and typeset.

PLEASE CITE THIS ARTICLE AS DOI: 10.1063/5.0123211

Accepted to Phys. Fluids 10.1063/5.0123211

- 536 ¹¹V. A. Sabelnikov, A. N. Lipatnikov, S. Nishiki, H. L. Dave, F. E. Hernández-Pérez, W. Song, and H.
537 G. Im, "Dissipation and dilatation rates in premixed turbulent flames," *Phys. Fluids* **33**, 035112
538 (2021).
- 539 ¹²N. Chakraborty, C. Kasten, U. Ahmed, and M. Klein, "Evolutions of strain rate and dissipation rate
540 of kinetic energy in turbulent premixed flames," *Phys. Fluids* **33**, 125132 (2021).
- 541 ¹³N. Chakraborty, U. Ahmed, M. Klein, and H. G. Im, "Alignment statistics of pressure Hessian with
542 strain rate tensor and reactive scalar gradient in turbulent premixed flames," *Phys. Fluids* **34**, 065120
543 (2022).
- 544 ¹⁴S. Kr. Ghai, N. Chakraborty, U. Ahmed and M. Klein, "Enstrophy evolution during head-on wall
545 interaction of premixed flames within turbulent boundary layers," *Phys. Fluids* **34**, 075124 (2022).
- 546 ¹⁵V. A. Sabelnikov, A. N. Lipatnikov, N. Nikitin, F. E. Hernández-Pérez, and H. G. Im, "Conditioned
547 structure functions in turbulent hydrogen/air flames," *Phys. Fluids* **34**, 085103 (2022).
- 548 ¹⁶A. N. Lipatnikov and J. Chomiak, "Effects of premixed flames on turbulence and turbulent scalar
549 transport," *Prog. Energy Combust. Sci.* **36**, 1-102 (2010).
- 550 ¹⁷V. A. Sabelnikov and A. N. Lipatnikov, "Recent advances in understanding of thermal expansion
551 effects in premixed turbulent flames," *Annu. Rev. Fluid Mech.* **49**, 91-117 (2017).
- 552 ¹⁸N. Chakraborty, "Influence of thermal expansion on fluid dynamics of turbulent premixed combustion
553 and its modeling implications," *Flow Turbul. Combust.* **106**, 753-848 (2021).
- 554 ¹⁹A.M. Steinberg, P. E. Hamlington, and X. Zhao, "Structure and dynamics of highly turbulent
555 premixed combustion," *Prog. Energy Combust. Sci.* **85**, 100900 (2021).
- 556 ²⁰S. H. R. Whitman, C. A. Z. Towery, A. Y. Poludnenko, and P. E. Hamlington, "Scaling and collapse
557 of conditional velocity structure functions in turbulent premixed flames," *Proc. Combust. Inst.* **37**,
558 2527-2535 (2019).
- 559 ²¹J. Lee, J. F. MacArt, and M. E. Mueller, "Heat release effects on the Reynolds stress budgets in
560 turbulent premixed jet flames at low and high Karlovitz numbers," *Combust. Flame* **216**, 1-8 (2020).
- 561 ²²R. Darragh, C. A. Z. Towery, A. Y. Poludnenko, and P. E. Hamlington, "Particle pair dispersion and
562 eddy diffusivity in a high-speed premixed flame," *Proc. Combust. Inst.* **38**, 2845-2852 (2021).
- 563 ²³J. Lee and M. E. Mueller, "Closure modeling for the conditional Reynolds stresses in turbulent
564 premixed combustion," *Proc. Combust. Inst.* **38**, 3031-3038 (2021).
- 565 ²⁴A. Kazbekov and A. M. Steinberg, "Flame- and flow-conditioned vorticity transport in premixed swirl
566 combustion," *Proc. Combust. Inst.* **38**, 2949-2956 (2021).
- 567 ²⁵A. Kazbekov and A. M. Steinberg, "Physical space analysis of cross-scale turbulent kinetic energy
568 transfer in premixed swirl flames," *Combust. Flame* **229**, 111403 (2021).
- 569 ²⁶K. N.C. Bray, "Turbulent transport in flames," *Proc. R. Soc. London A* **451**, 231-256 (1995).
- 570 ²⁷D. Veynante, A. Trounev, K. N. C. Bray, and T. Mantel, "Gradient and counter-gradient scalar
571 transport in turbulent premixed flames," *J. Fluid Mech.* **332**, 263-293.
- 572 ²⁸R. W. Bilger, "Some aspects of scalar dissipation," *Flow, Turbul. Combust.* **72**, 93-114 (2004).
- 573 ²⁹A. S. Monin and A. M. Yaglom, *Statistical Fluid Mechanics: Mechanics of Turbulence* (The MIT
574 Press, Cambridge, Massachusetts, 1975), Vol. 2.
- 575 ³⁰J. F. MacArt, T. Genga, and M. E. Mueller, "Effects of combustion heat release on velocity and
576 scalar statistics in turbulent premixed jet flames at low and high Karlovitz numbers," *Combust. Flame*
577 **191**, 468-485 (2018).
- 578 ³¹J. F. MacArt, T. Genga, and M. E. Mueller, "Evolution of flame-conditioned velocity statistics in
579 turbulent premixed jet flames at varying Karlovitz number," *Proc. Combust. Inst.* **37**, 2503-2510
580 (2019).
- 581 ³²J. O'Brien, C. A. Z. Towery, P. E. Hamlington, M. Ihme, A. Y. Poludnenko, and J. Urzay, "The cross-
582 scale physical-space transfer of kinetic energy in turbulent premixed flames," *Proc. Combust. Inst.*
583 **36**, 1967-1975 (2017).
- 584 ³³A. J. Chorin and J. E. Marsden, *A Mathematical Introduction to Fluid Mechanics* (Springer, Berlin,
585 Germany, 1993).
- 586 ³⁴V. A. Sabelnikov, R. Yu, and A. N. Lipatnikov, "Thin reaction zones in constant-density turbulent
587 flows at low Damköhler numbers: Theory and simulations," *Phys. Fluids* **31**, 055104 (2019).

This is the author's peer reviewed, accepted manuscript. However, the online version of record will be different from this version once it has been copyedited and typeset.

PLEASE CITE THIS ARTICLE AS DOI: 10.1063/5.0123211

Accepted to Phys. Fluids 10.1063/5.0123211

- 588 ³⁵J. F. Driscoll, J. H. Chen, A. W. Skiba, C. D. Carter, E. R. Hawkes, and H. Wang, "Premixed flames
589 subjected to extreme turbulence: Some questions and recent answers," *Prog. Energy Combust. Sci.*
590 **76**, 100802, (2020).
- 591 ³⁶N. Swaminathan, R. W. Bilger, and B. Cuenot, "Relationship between turbulent scalar flux and
592 conditional dilatation in premixed flames with complex chemistry," *Combust. Flame* **126**, 1764-1779
593 (2001).
- 594 ³⁷N. Chakraborty and R. S. Cant, "Effects of Lewis number on scalar transport in turbulent premixed
595 flames," *Phys. Fluids* **21**, 035110 (2009).
- 596 ³⁸A. N. Lipatnikov and J. Chomiak, "Molecular transport effects on turbulent flame propagation and
597 structure," *Prog. Energy Combust. Sci.* **31**, 1-73 (2005).
- 598 ³⁹A. N. Lipatnikov and J. Chomiak, "Turbulent flame speed and thickness: Phenomenology, evaluation,
599 and application in multi-dimensional simulations," *Prog. Energy Combust. Sci.* **28**, 1-73 (2002).
- 600 ⁴⁰T. Sponfeldner, N. Souloupoulos, F. Beyrau, Y. Hardalupas, A. M. K. P. Taylor, and J. C. Vassilicos,
601 "The structure of turbulent flames in fractal- and regular-grid-generated turbulence," *Combust. Flame*
602 **162**, 3379-3393 (2015).
- 603 ⁴¹J. Kim, A. Satja, R. P. Lucht, and J. P. Gore, "Effects of turbulent flow regime on perforated plate
604 stabilized piloted lean premixed flames", *Combust. Flame* **211**, 158-172 (2020).
- 605 ⁴²S. Kheirkhah and Ö. L. Gülder, "A revisit to the validity of flamelet assumptions in turbulent
606 premixed combustion and implications for future research," *Combust. Flame* **239**, 111635 (2022).
- 607 ⁴³R. Yu, X.-S. Bay, and A. N. Lipatnikov, "A direct numerical simulation study of interface propagation
608 in homogeneous turbulence," *J. Fluid Mech.* **772**, 127-164 (2015).
- 609 ⁴⁴R. Yu and A.N. Lipatnikov, "Direct numerical simulation study of statistically stationary propagation
610 of a reaction wave in homogeneous turbulence," *Phys. Rev. E* **95**, 063101 (2017).
- 611 ⁴⁵T. Kulkarni and F. Bisetti, "Analysis of the development of the flame brush in turbulent premixed
612 spherical flames," *Combust. Flame* **234**, 111640 (2021).
- 613 ⁴⁶D. H. Wacks, N. Chakraborty, M. Klein, P. G. Arias, and H. G. Im, "Flow topologies in different
614 regimes of premixed turbulent combustion: A direct numerical simulation analysis," *Phys. Rev. Fluids*
615 **1**, 083401 (2016).
- 616 ⁴⁷A. N. Lipatnikov, V. A. Sabelnikov, F. E. Hernández-Pérez, W. Song, and H. G. Im, "A priori DNS
617 study of applicability of flamelet concept to predicting mean concentrations of species in turbulent
618 premixed flames at various Karlovitz numbers," *Combust. Flame* **222**, 370-382 (2020).
- 619 ⁴⁸A. N. Lipatnikov, V. A. Sabelnikov, F. E. Hernández-Pérez, W. Song, and H. G. Im, "Prediction of
620 mean radical concentrations in lean hydrogen-air turbulent flames at different Karlovitz numbers
621 adopting a newly extended flamelet-based presumed PDF," *Combust. Flame* **226**, 248-259 (2021).
- 622 ⁴⁹M. P. Burke, M. Chaos, Y. Ju, F. L. Dryer, and S. J. Klippenstein, "Comprehensive H₂/O₂ kinetic
623 model for high-pressure combustion," *Int. J. Chem. Kinet.* **44**, 444-474 (2012).
- 624 ⁵⁰J. H. Chen and H. G. Im, "Stretch effects on the burning velocity of turbulent premixed hydrogen-air
625 flames," *Proc. Combust. Inst.* **28**, 211-218 (2000).
- 626 ⁵¹H. G. Im and J. H. Chen, "Preferential diffusion effects on the burning rate of interacting turbulent
627 premixed hydrogen-air flames," *Combust. Flame* **131**, 246-258 (2002).
- 628 ⁵²T. Passot and A. Pouquet, "Numerical simulation of compressible homogeneous flows in the turbulent
629 regime," *J. Fluid Mech.* **181**, 441-466 (1987).
- 630 ⁵³H. Bhatia, G. Norgard, V. Pascucci, and P.-T. Bremer, "The Helmholtz-Hodge decomposition – a
631 survey," *IEEE Trans. Vis. Comput. Graph.* **19**, 1386-1404 (2013).
- 632 ⁵⁴H. Bhatia, V. Pascucci, and P.-T. Bremer, "The natural Helmholtz-Hodge decomposition for open-
633 boundary flow analysis," *IEEE Trans. Vis. Comput. Graph.* **20**, 1566-1578 (2014).
- 634 ⁵⁵V. A. Sabelnikov, A. N. Lipatnikov, N. Nikitin, S. Nishiki, and T. Hasegawa, "Application of
635 Helmholtz-Hodge decomposition and conditioned structure functions to exploring influence of
636 premixed combustion on turbulence upstream of the flame," *Proc. Combust. Inst.* **38**, 3077-3085
637 (2021).
- 638 ⁵⁶V. A. Sabelnikov, A. N. Lipatnikov, N. Nikitin, S. Nishiki, and T. Hasegawa, "Solenoidal and
639 potential velocity fields in weakly turbulent premixed flames," *Proc. Combust. Inst.* **38**, 3087-3095
640 (2021).

This is the author's peer reviewed, accepted manuscript. However, the online version of record will be different from this version once it has been copyedited and typeset.

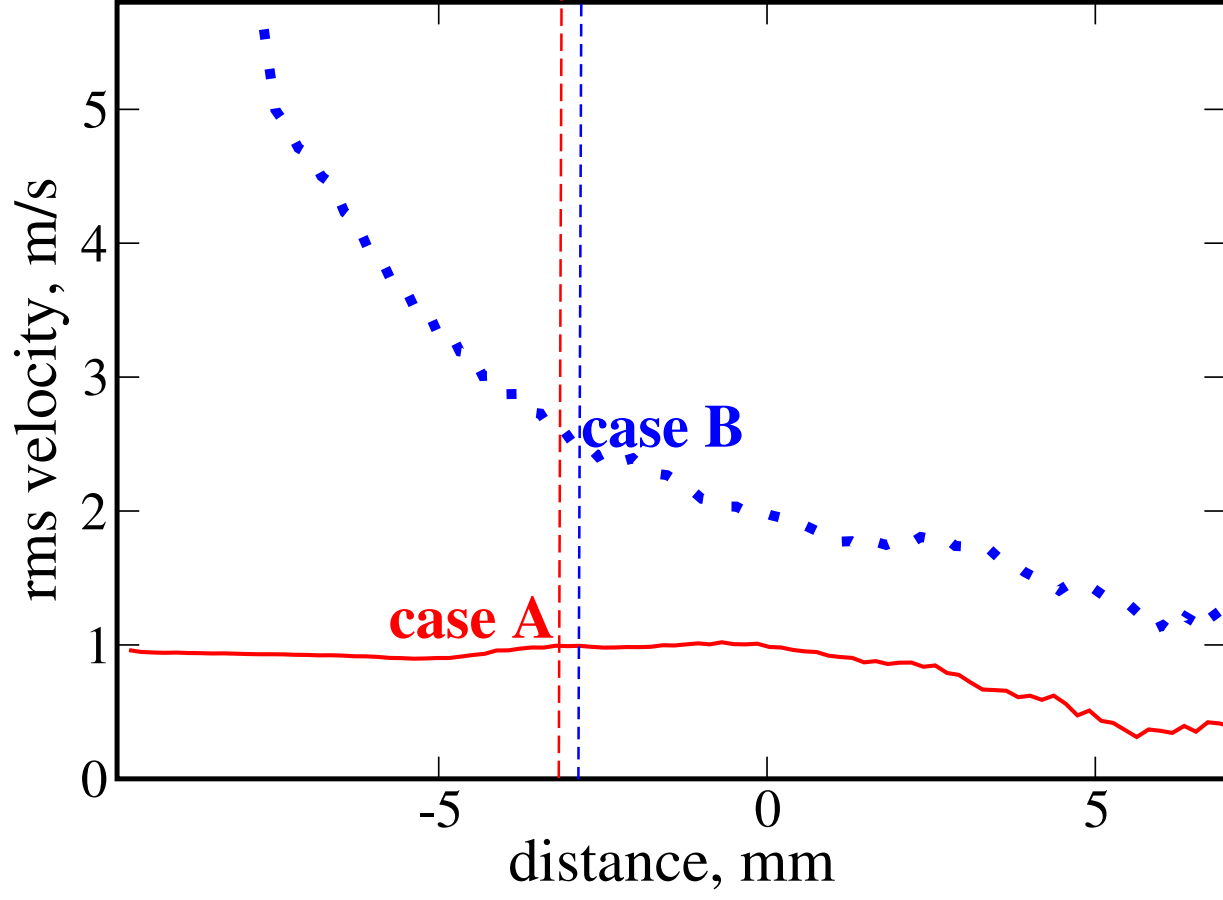
PLEASE CITE THIS ARTICLE AS DOI: 10.1063/5.0123211

Accepted to Phys. Fluids 10.1063/5.0123211

- 641 ⁵⁷R. Yu, T. Nillson, X.-S. Bai, and A. N. Lipatnikov, "Evolution of averaged local premixed flame
642 thickness in a turbulent flow," *Combust. Flame* **207**, 232-249 (2019).
- 643 ⁵⁸L. D. Landau and E. M. Lifshitz, *Fluid Mechanics* (Pergamon Press, Oxford, 1987).
- 644 ⁵⁹Ya. B. Zel'dovich, G. I. Barenblatt, V. B. Librovich, and G. M. Makhviladze, *The Mathematical*
645 *Theory of Combustion and Explosions* (Consultants Bureau, New York, 1985).
- 646 ⁶⁰R. Borghi, "On the structure and morphology of turbulent premixed flames," in *Recent Advances in*
647 *Aerospace Science*, edited by S. Casci and C. Bruno (Plenum, New York, 1984), pp. 117-138.
- 648 ⁶¹F. A. Williams, *Combustion Theory*, 2nd ed. (Benjamin/Cummings, Menlo Park, California, 1985).
- 649 ⁶²N. Peters, "Laminar flamelet concepts in turbulent combustion," *Proc. Combust. Inst.* **21**, 1231
650 (1986).
- 651 ⁶³S. Corrsin, "Reactant concentration spectrum in turbulent mixing with a first-order reaction," *J. Fluid*
652 *Mech.* **11**, 407-416 (1961).
- 653 ⁶⁴A. N. Lipatnikov and V. A. Sabelnikov, "Karlovitz numbers and premixed turbulent combustion
654 regimes for complex-chemistry flames," *Energies* **15**, 5840 (2022).
- 655 ⁶⁵H. Kolla, E. R. Hawkes, A. R. Kerstein, N. Swaminathan, and J. H. Chen, "On velocity and reactive
656 scalar spectra in turbulent premixed flames," *J. Fluid Mech.* **754**, 456 (2014).
- 657 ⁶⁶A. N. Lipatnikov, J. Chomiak, V. A. Sabelnikov, S. Nishiki, and T. Hasegawa, "Influence of heat
658 release in a premixed flame on weakly turbulent flow of unburned gas: a DNS Study," in *Proceedings*
659 *of the 25th International Colloquium on the Dynamics of Explosions and Reactive Systems, 2-7 August*
660 *2015, Leeds, UK*, edited by M.I. Radulescu (University of Leeds, UK, 2015), paper 74.
- 661 ⁶⁷C. A. Z. Towery, A. Y. Poludnenko, J. Urzay, J. O'Brien, M. Ihme, and P. E. Hamlington, "Spectral
662 kinetic energy transfer in turbulent premixed reacting flows," *Phys. Rev. E* **93**, 053115 (2016).
- 663 ⁶⁸H. Boughanem and A. Trouvé, "The domain of influence of flame instabilities in turbulent premixed
664 combustion," *Proc. Combust. Inst.* **27**, 971-978 (1998).
- 665 ⁶⁹S. Chaudhuri, V. Akkerman, and C. K. Law, "Spectral formulation of turbulent flame speed with
666 consideration of hydrodynamic instability," *Phys. Rev. E* **84**, 026322 (2011).
- 667 ⁷⁰N. Fogla, F. Creta, and M. Matalon, "The turbulent flame speed for low-to-moderate turbulence
668 intensities: Hydrodynamic theory vs. experiments," *Combust. Flame* **175**, 155-169 (2017).
- 669 ⁷¹H. G. Im, P. G. Arias, S. Chaudhuri, and H. A. Uraakara, "Direct numerical simulations of
670 statistically stationary turbulent premixed flames," *Combust. Sci. Technol.* **188**, 1182 (2016).
- 671 ⁷²C. S. Yoo, Y. Wang, A. Trouve, and H. G. Im, "Characteristic boundary conditions for direct
672 simulations of turbulent counterflow flames," *Combust. Theor. Model.* **9**, 617 (2005).
- 673 ⁷³R. S. Rogallo, Numerical Experiments in Homogeneous Turbulence, NASA Technical Memorandum
674 81315, NASA Ames Research Center, California, 1981.

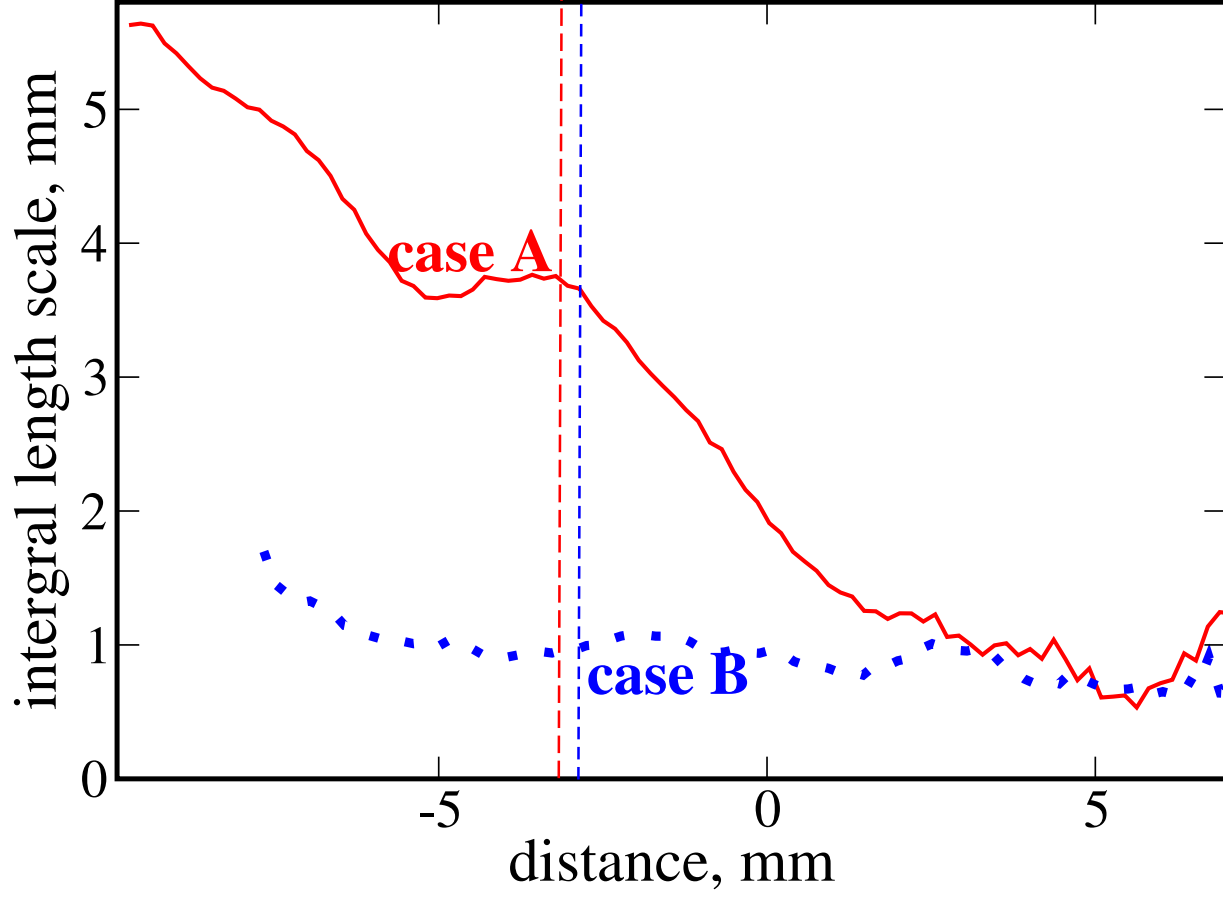
This is the author's peer reviewed, accepted manuscript. However, the online version of record will be different from this version once it has been copyedited and typeset.

PLEASE CITE THIS ARTICLE AS DOI: 10.1063/5.0123211



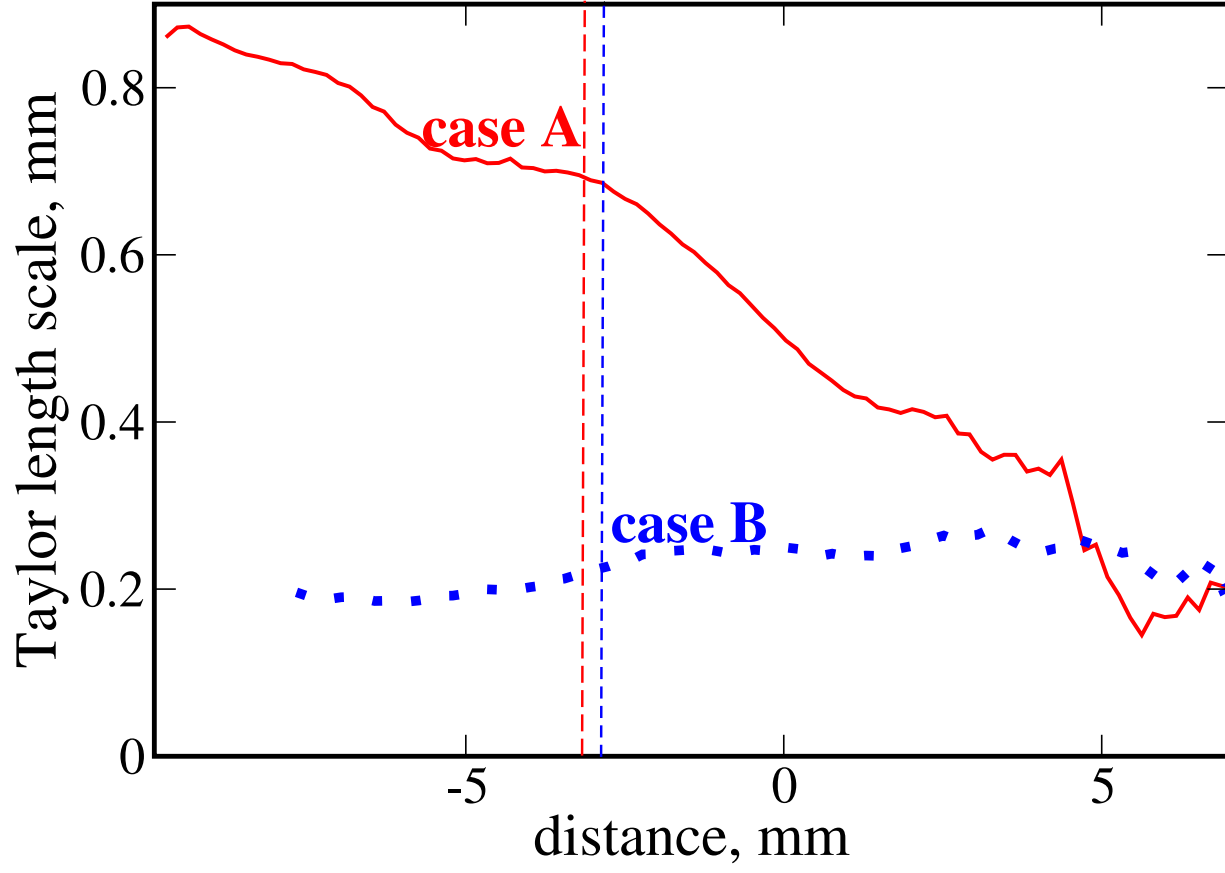
This is the author's peer reviewed, accepted manuscript. However, the online version of record will be different from this version once it has been copyedited and typeset.

PLEASE CITE THIS ARTICLE AS DOI: 10.1063/5.0123211



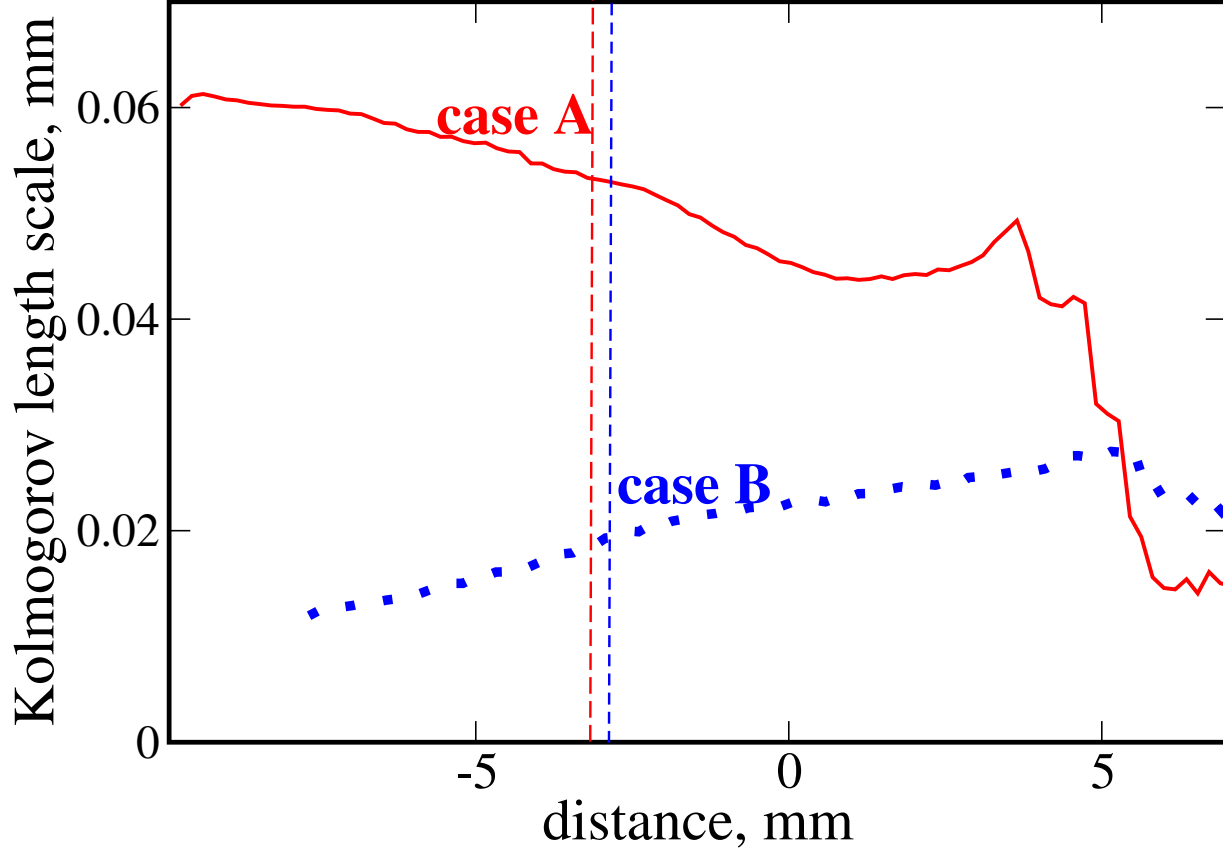
This is the author's peer reviewed, accepted manuscript. However, the online version of record will be different from this version once it has been copyedited and typeset.

PLEASE CITE THIS ARTICLE AS DOI: 10.1063/5.0123211



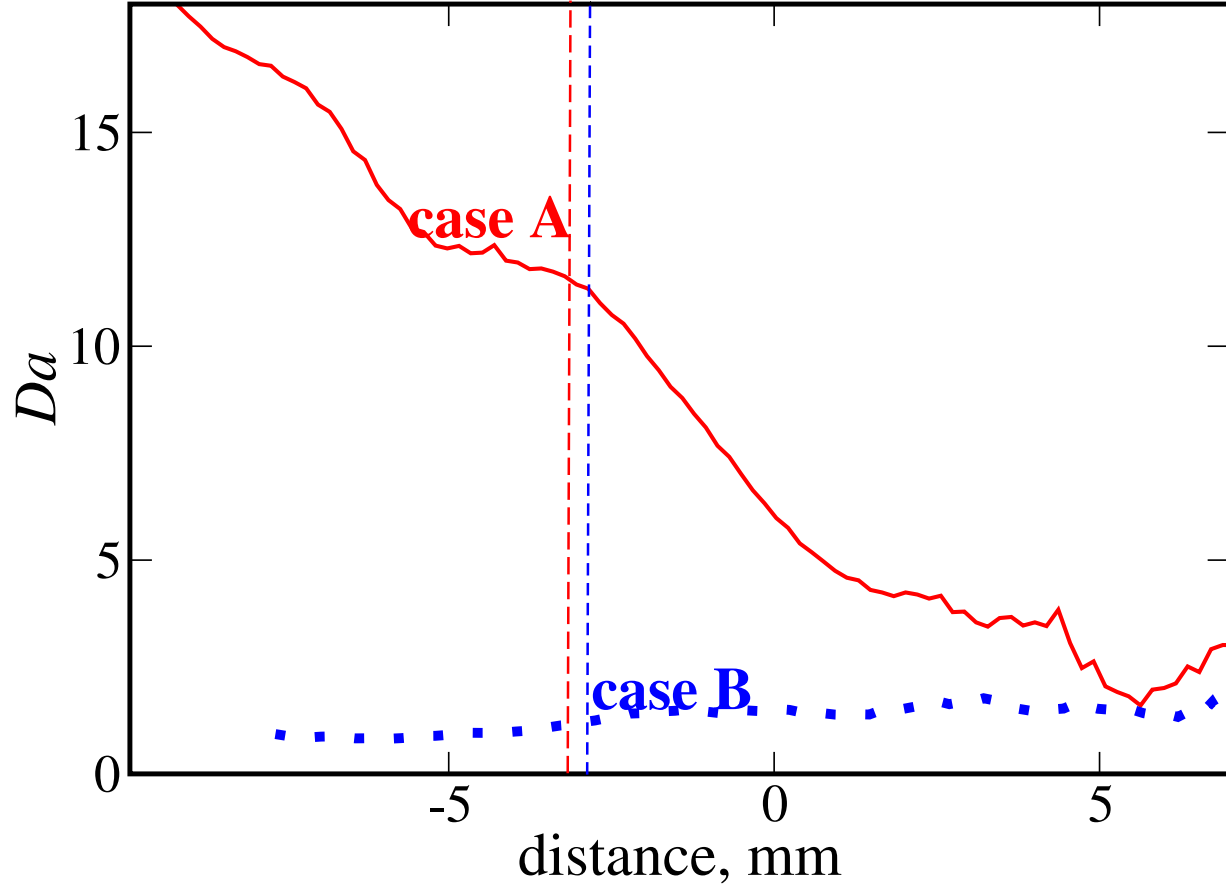
This is the author's peer reviewed, accepted manuscript. However, the online version of record will be different from this version once it has been copyedited and typeset.

PLEASE CITE THIS ARTICLE AS DOI: 10.1063/5.0123211



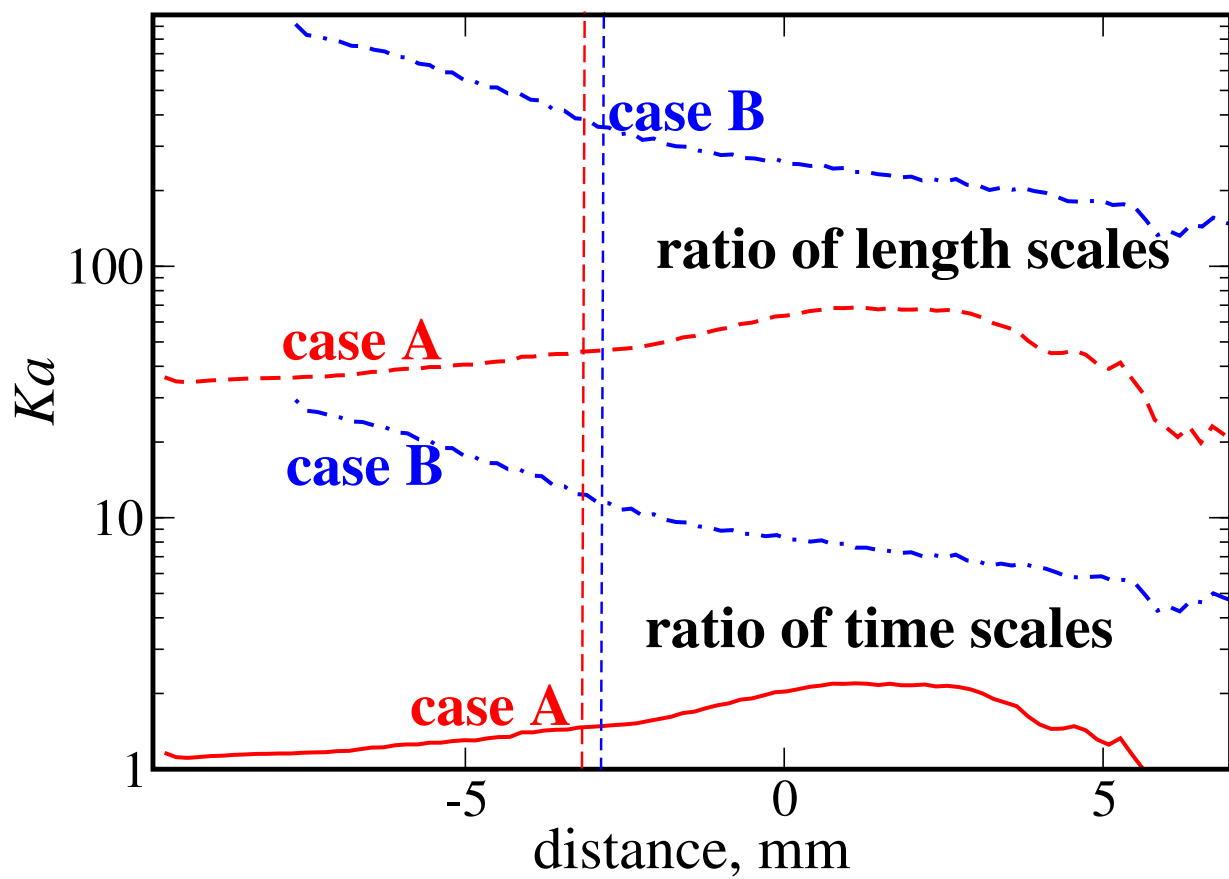
This is the author's peer reviewed, accepted manuscript. However, the online version of record will be different from this version once it has been copyedited and typeset.

PLEASE CITE THIS ARTICLE AS DOI: 10.1063/5.0123211



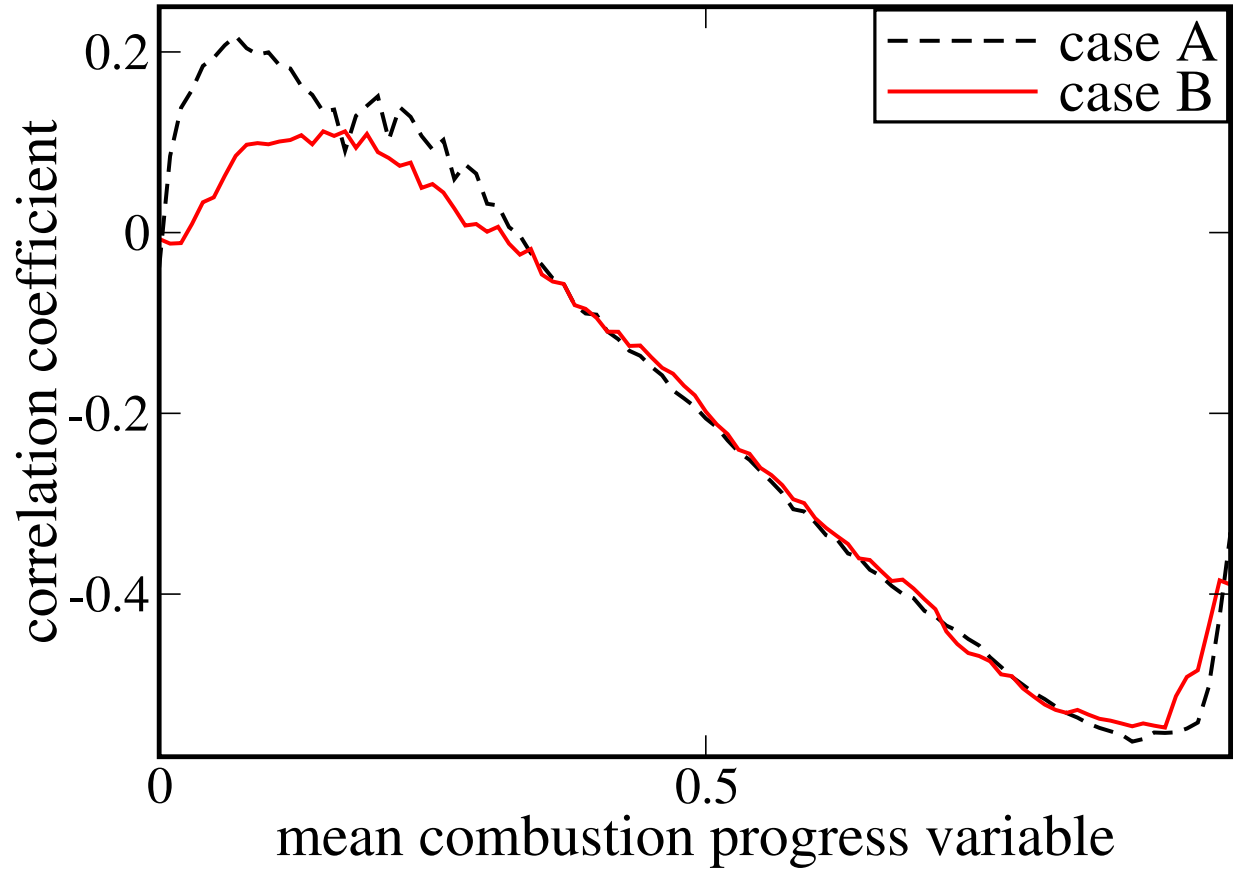
This is the author's peer reviewed, accepted manuscript. However, the online version of record will be different from this version once it has been copyedited and typeset.

PLEASE CITE THIS ARTICLE AS DOI: 10.1063/5.0123211



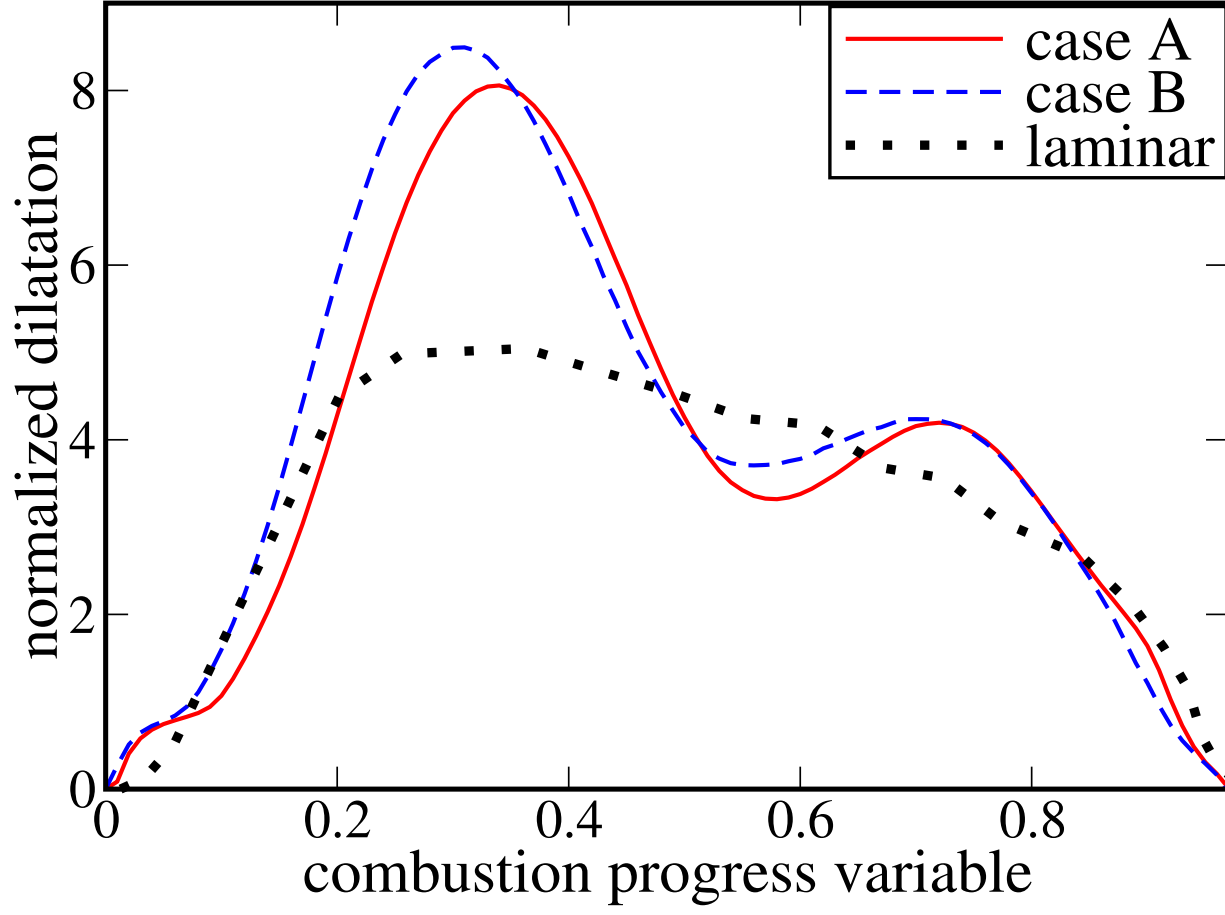
This is the author's peer reviewed, accepted manuscript. However, the online version of record will be different from this version once it has been copyedited and typeset.

PLEASE CITE THIS ARTICLE AS DOI: 10.1063/5.0123211



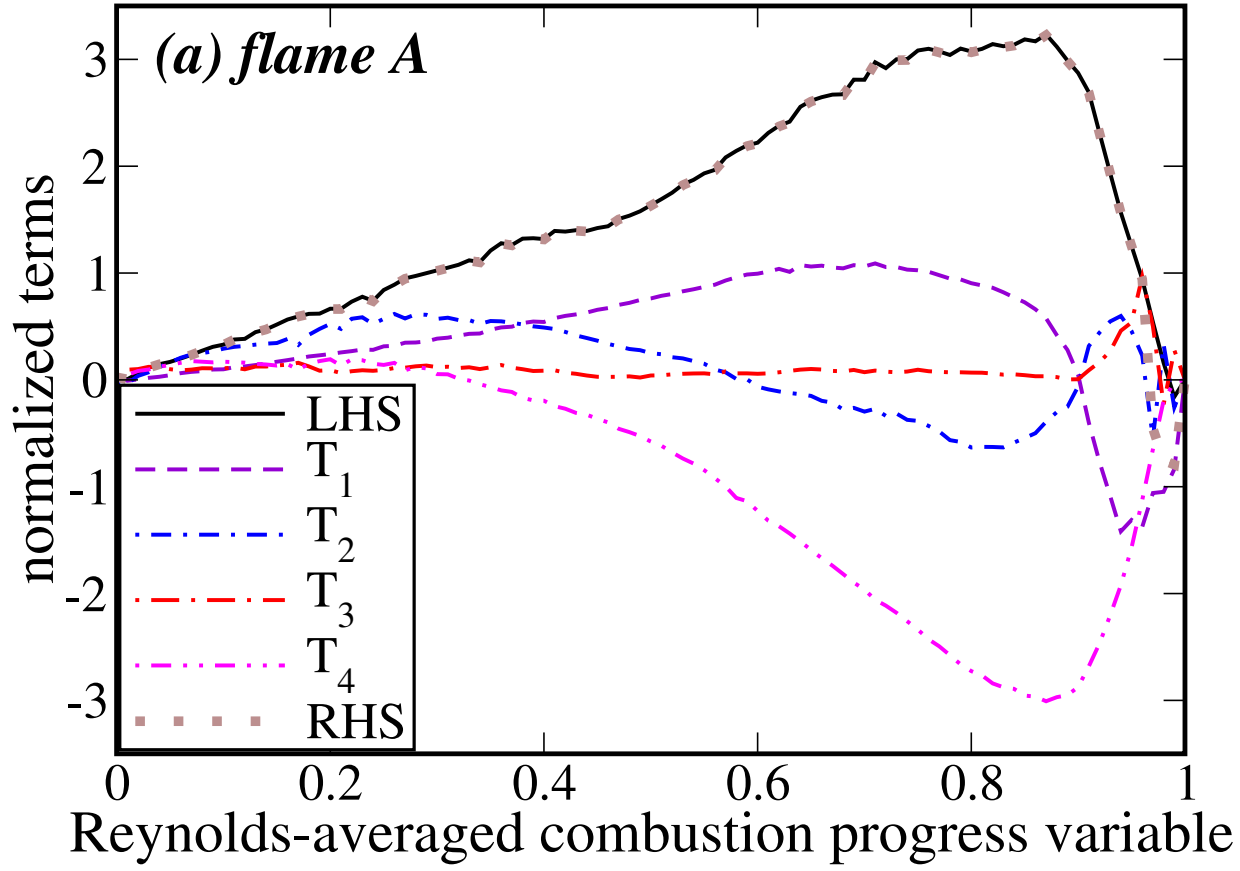
This is the author's peer reviewed, accepted manuscript. However, the online version of record will be different from this version once it has been copyedited and typeset.

PLEASE CITE THIS ARTICLE AS DOI: 10.1063/5.0123211



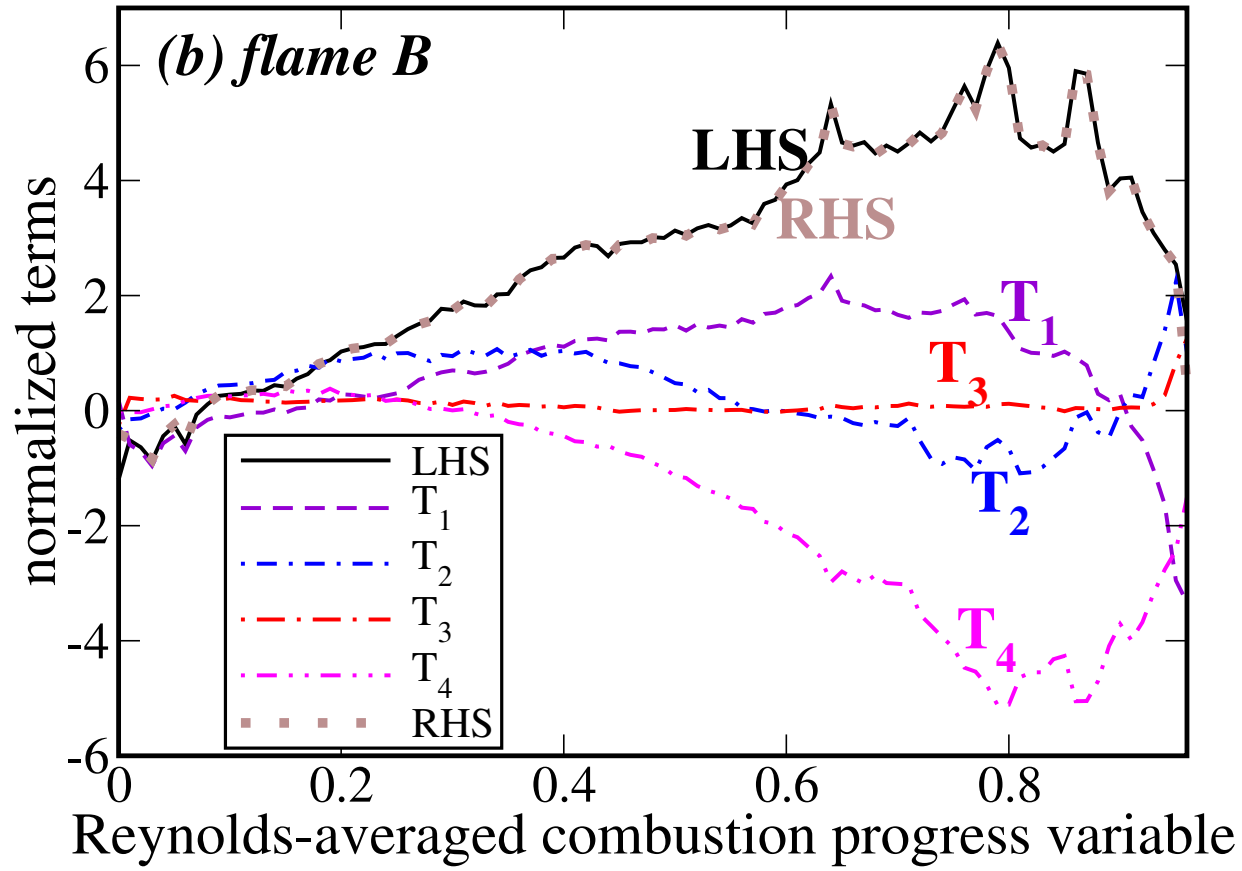
This is the author's peer reviewed, accepted manuscript. However, the online version of record will be different from this version once it has been copyedited and typeset.

PLEASE CITE THIS ARTICLE AS DOI: 10.1063/5.0123211



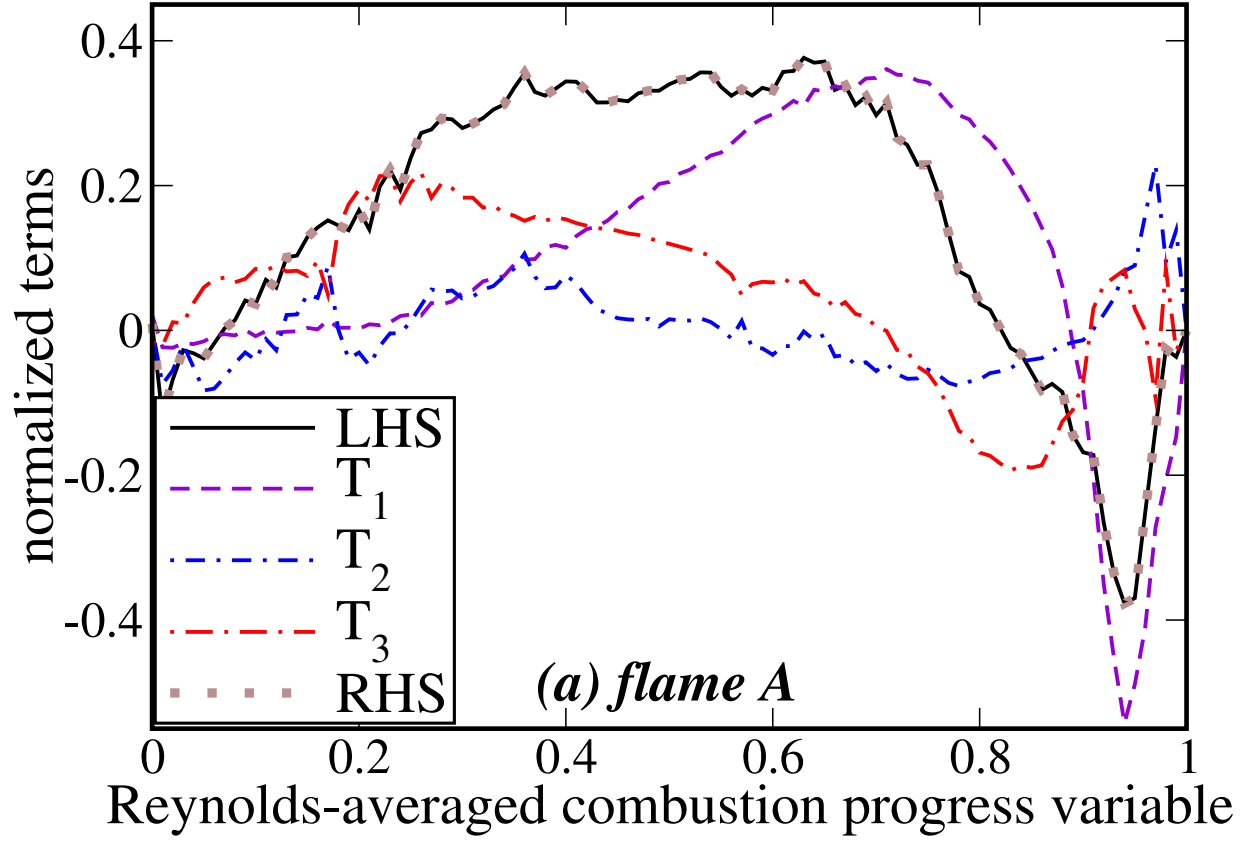
This is the author's peer reviewed, accepted manuscript. However, the online version of record will be different from this version once it has been copyedited and typeset.

PLEASE CITE THIS ARTICLE AS DOI: 10.1063/5.0123211



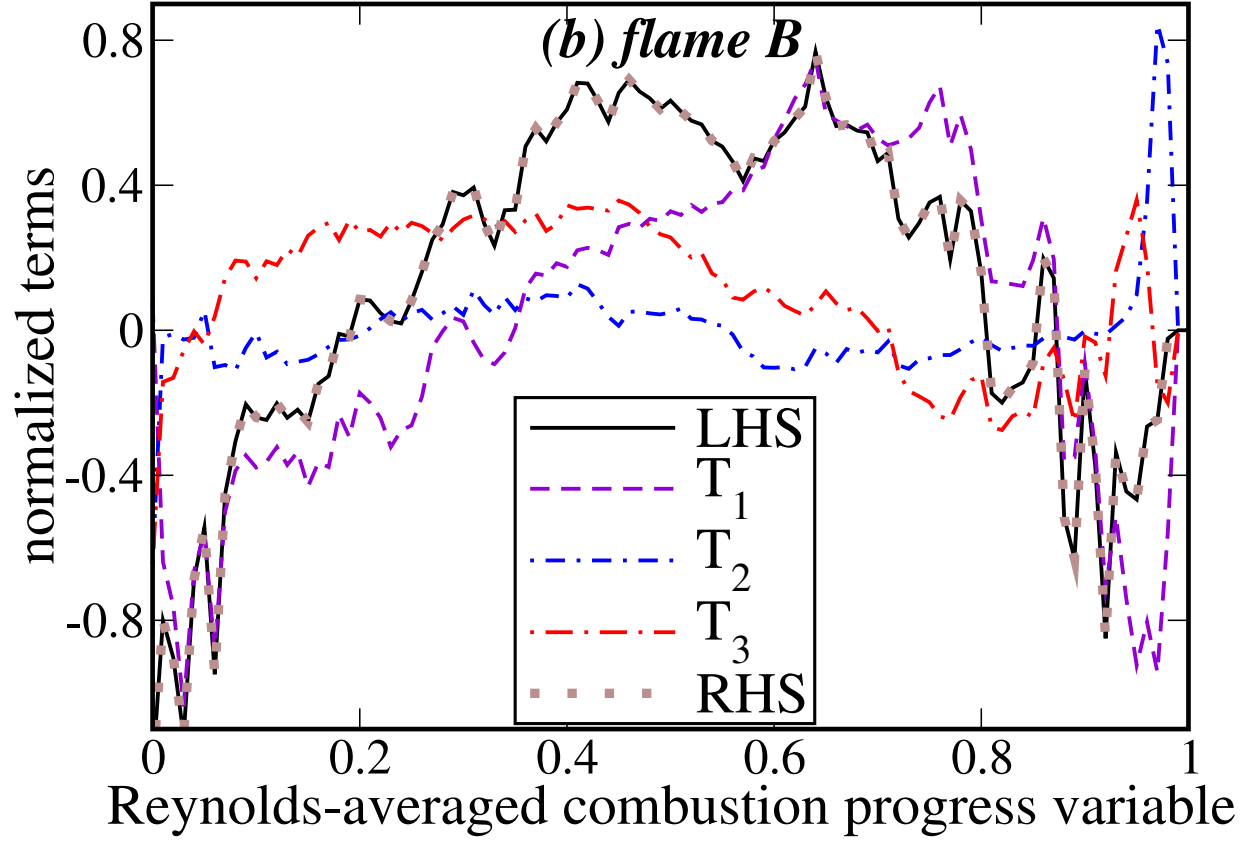
This is the author's peer reviewed, accepted manuscript. However, the online version of record will be different from this version once it has been copyedited and typeset.

PLEASE CITE THIS ARTICLE AS DOI: 10.1063/5.0123211



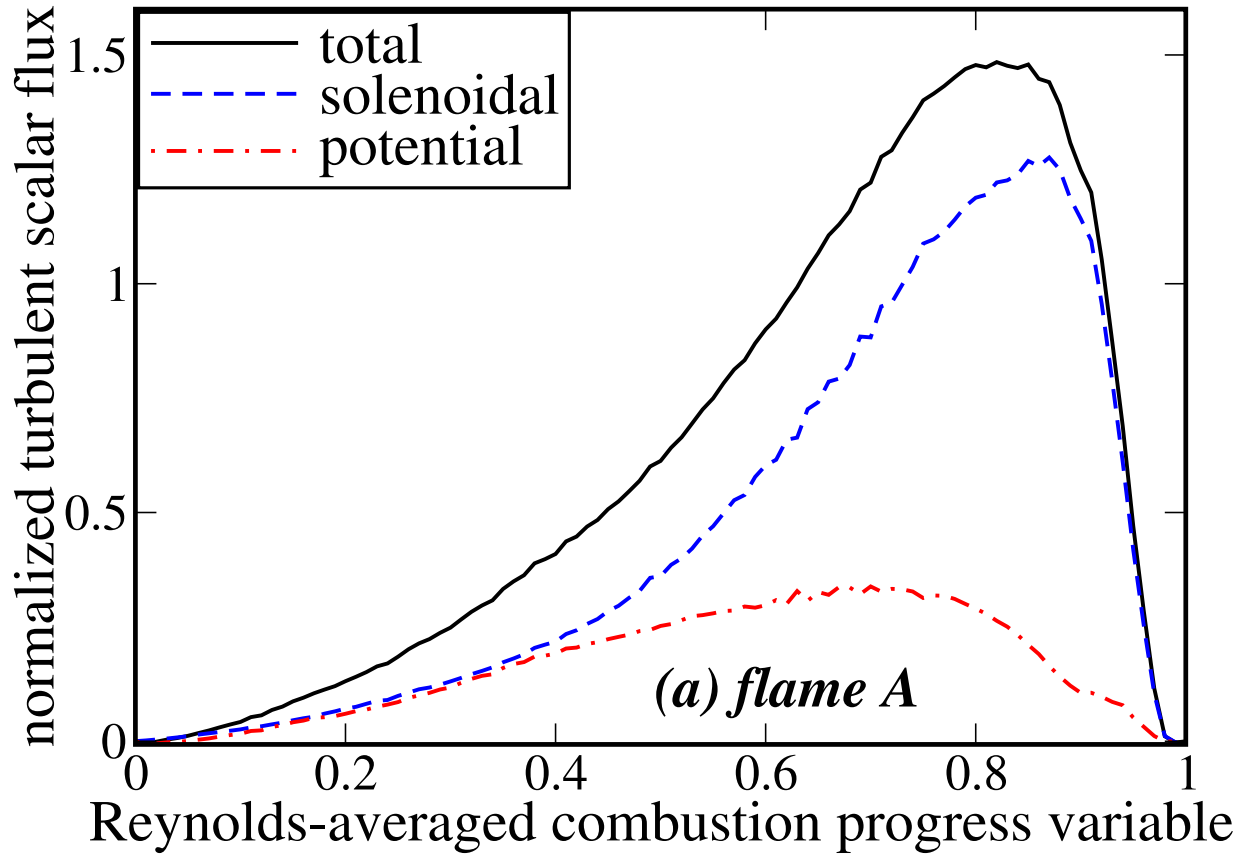
This is the author's peer reviewed, accepted manuscript. However, the online version of record will be different from this version once it has been copyedited and typeset.

PLEASE CITE THIS ARTICLE AS DOI: 10.1063/5.0123211



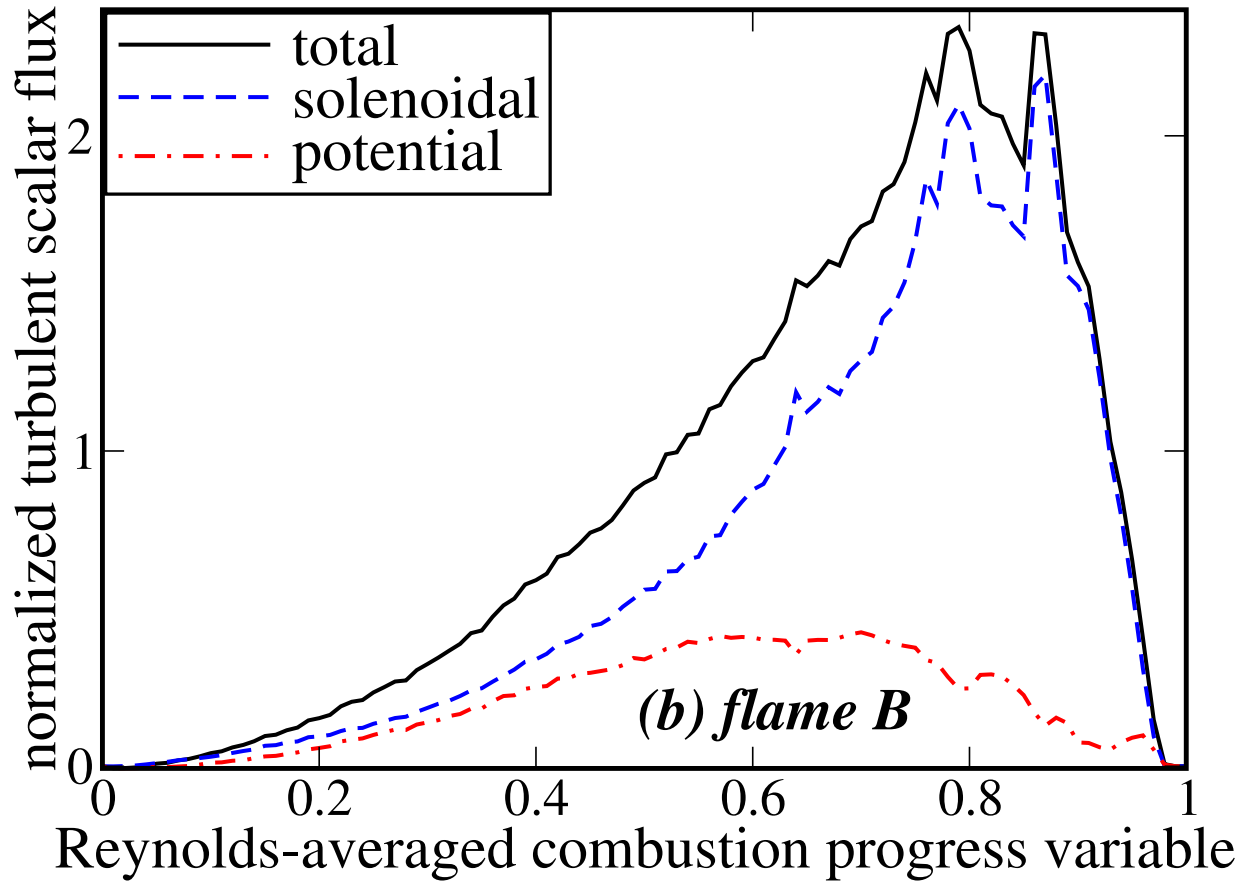
This is the author's peer reviewed, accepted manuscript. However, the online version of record will be different from this version once it has been copyedited and typeset.

PLEASE CITE THIS ARTICLE AS DOI: 10.1063/5.0123211



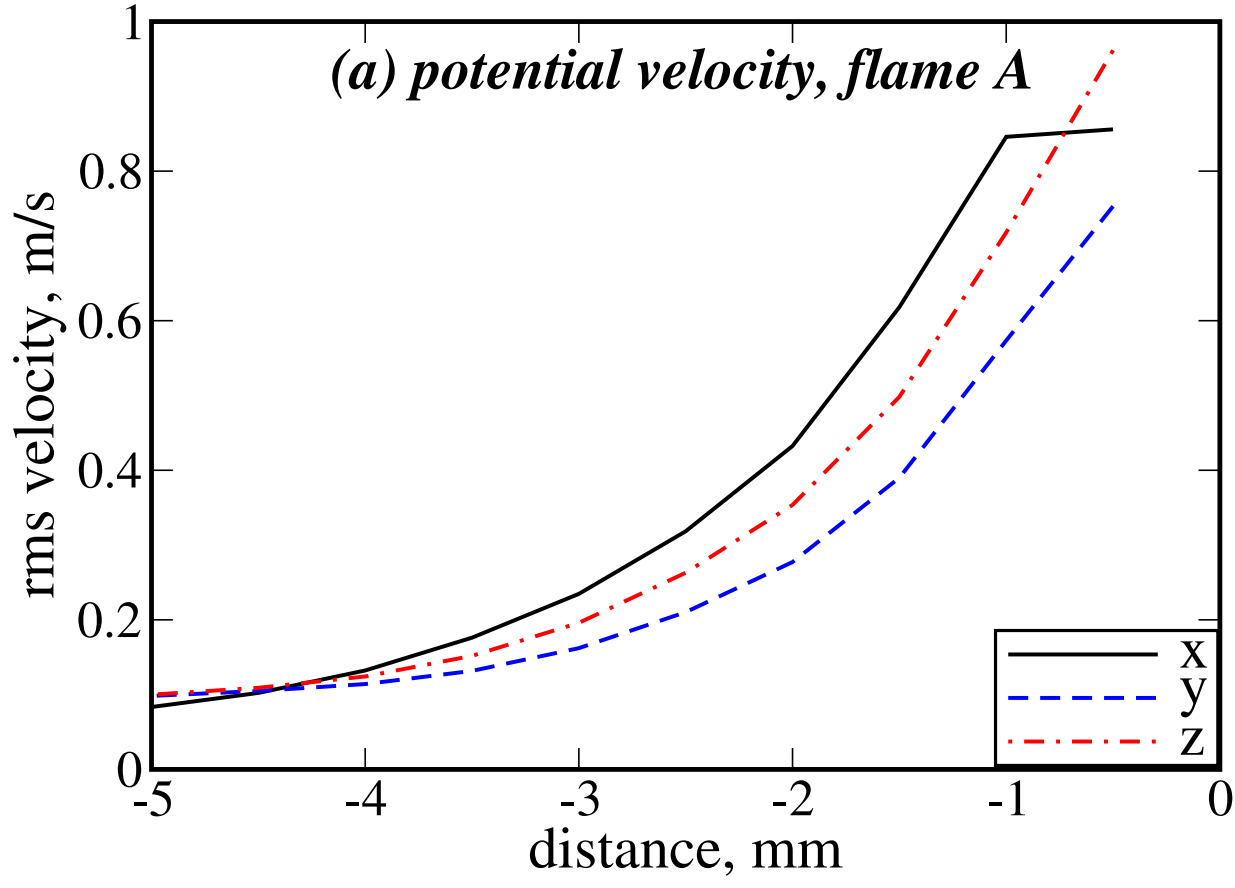
This is the author's peer reviewed, accepted manuscript. However, the online version of record will be different from this version once it has been copyedited and typeset.

PLEASE CITE THIS ARTICLE AS DOI: 10.1063/5.0123211



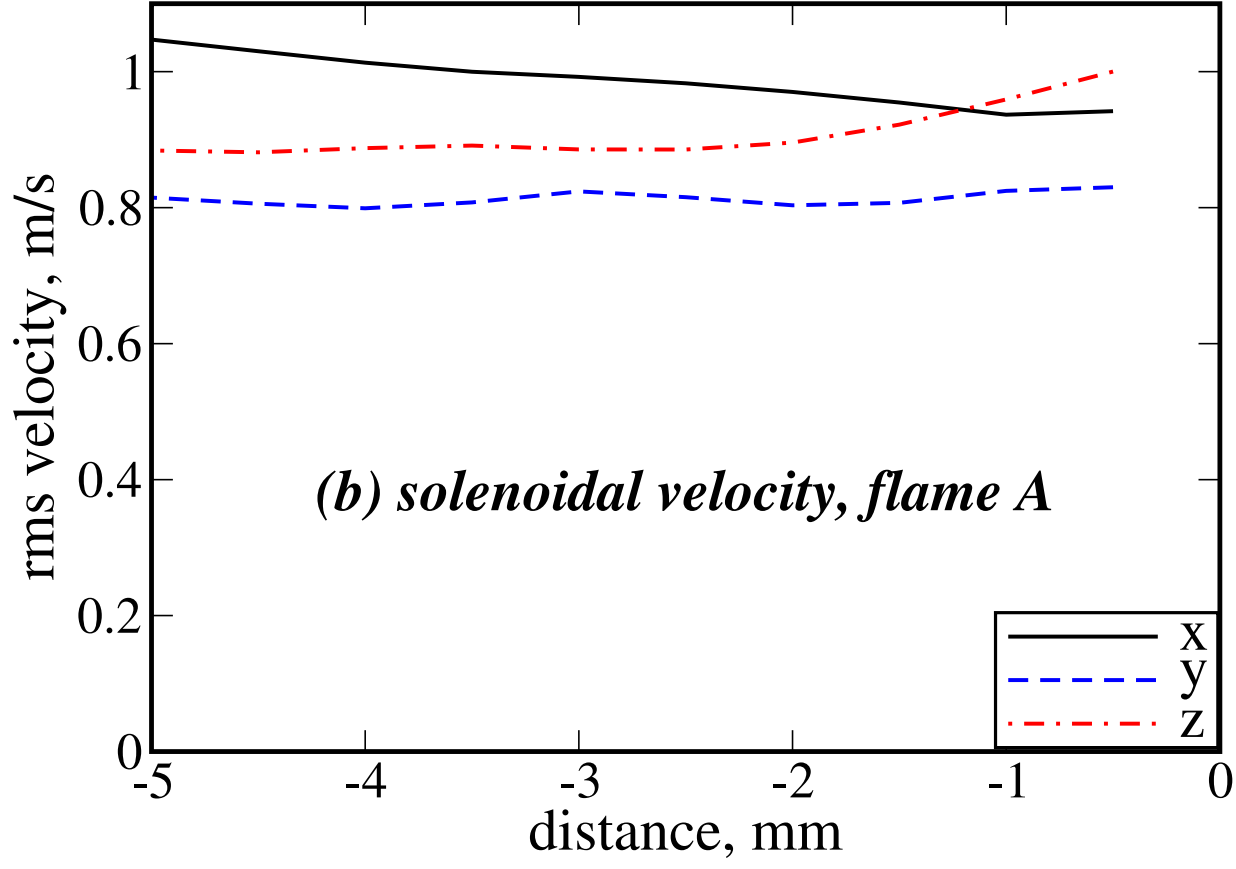
This is the author's peer reviewed, accepted manuscript. However, the online version of record will be different from this version once it has been copyedited and typeset.

PLEASE CITE THIS ARTICLE AS DOI: 10.1063/5.0123211



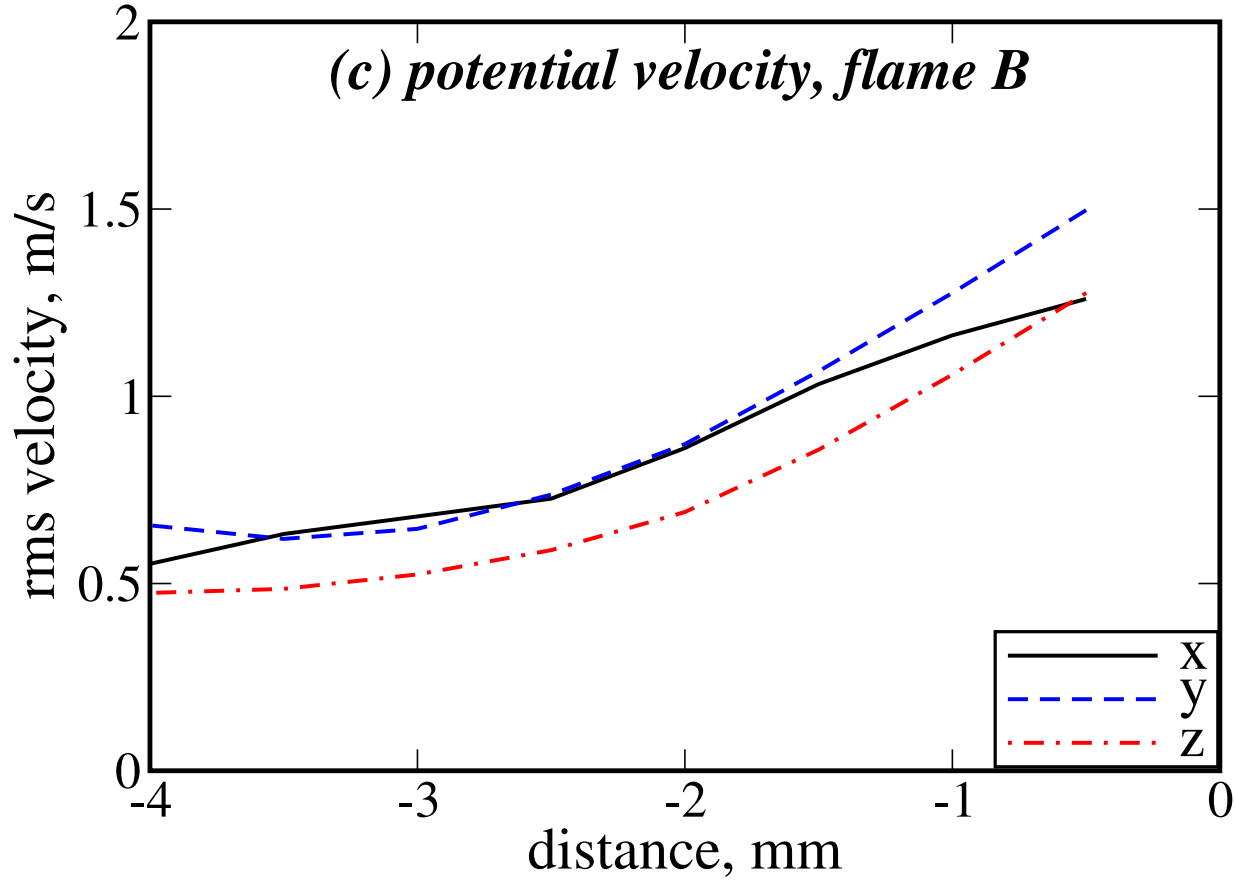
This is the author's peer reviewed, accepted manuscript. However, the online version of record will be different from this version once it has been copyedited and typeset.

PLEASE CITE THIS ARTICLE AS DOI: 10.1063/5.0123211



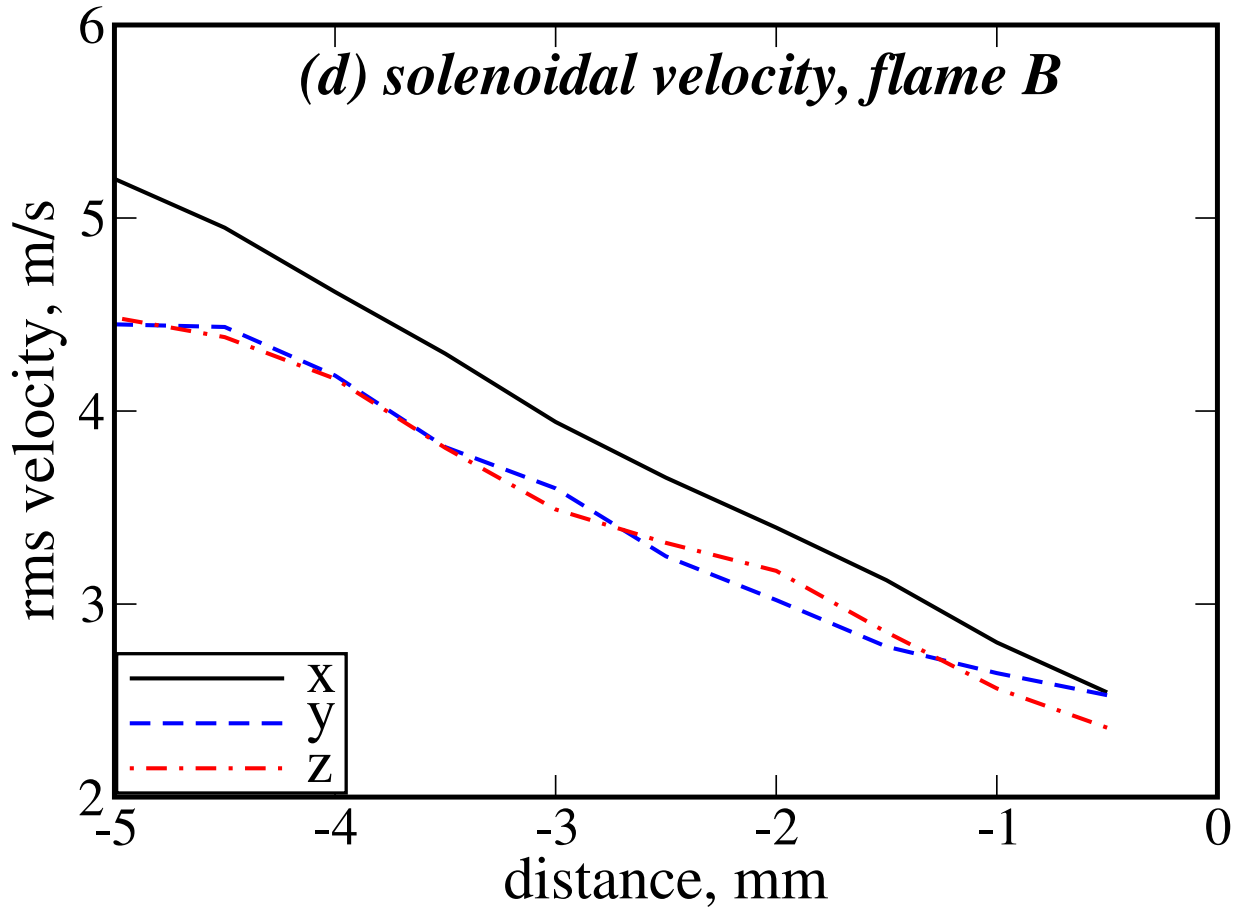
This is the author's peer reviewed, accepted manuscript. However, the online version of record will be different from this version once it has been copyedited and typeset.

PLEASE CITE THIS ARTICLE AS DOI: 10.1063/5.0123211



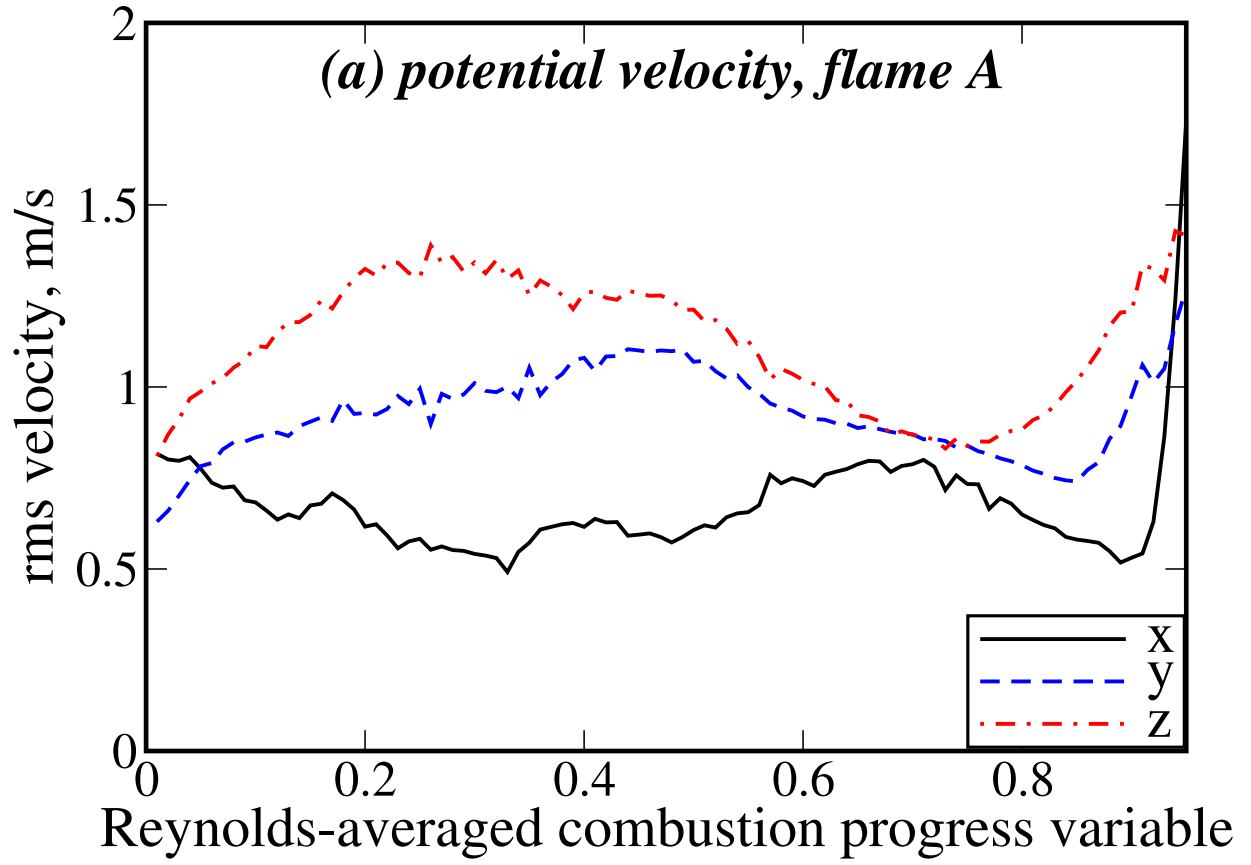
This is the author's peer reviewed, accepted manuscript. However, the online version of record will be different from this version once it has been copyedited and typeset.

PLEASE CITE THIS ARTICLE AS DOI: 10.1063/5.0123211



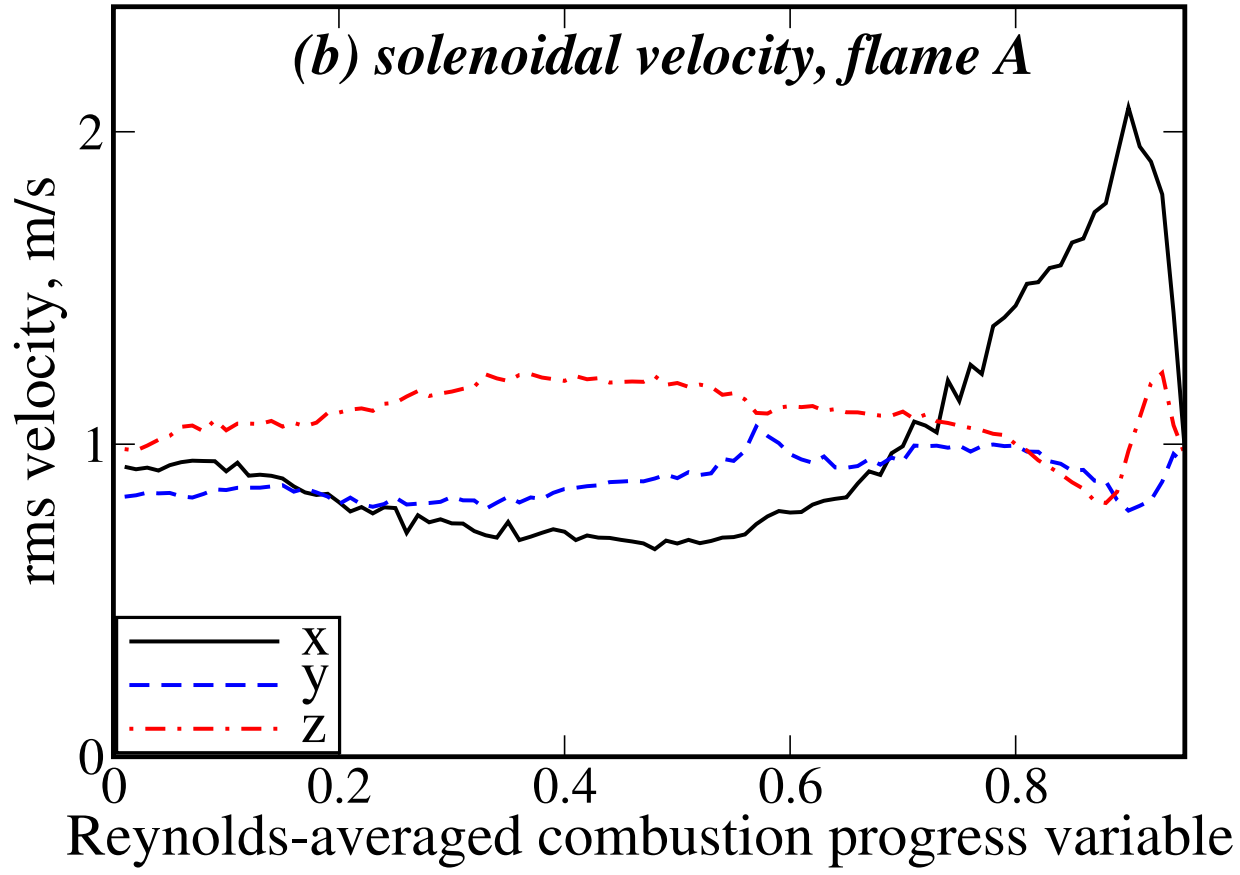
This is the author's peer reviewed, accepted manuscript. However, the online version of record will be different from this version once it has been copyedited and typeset.

PLEASE CITE THIS ARTICLE AS DOI: 10.1063/5.0123211



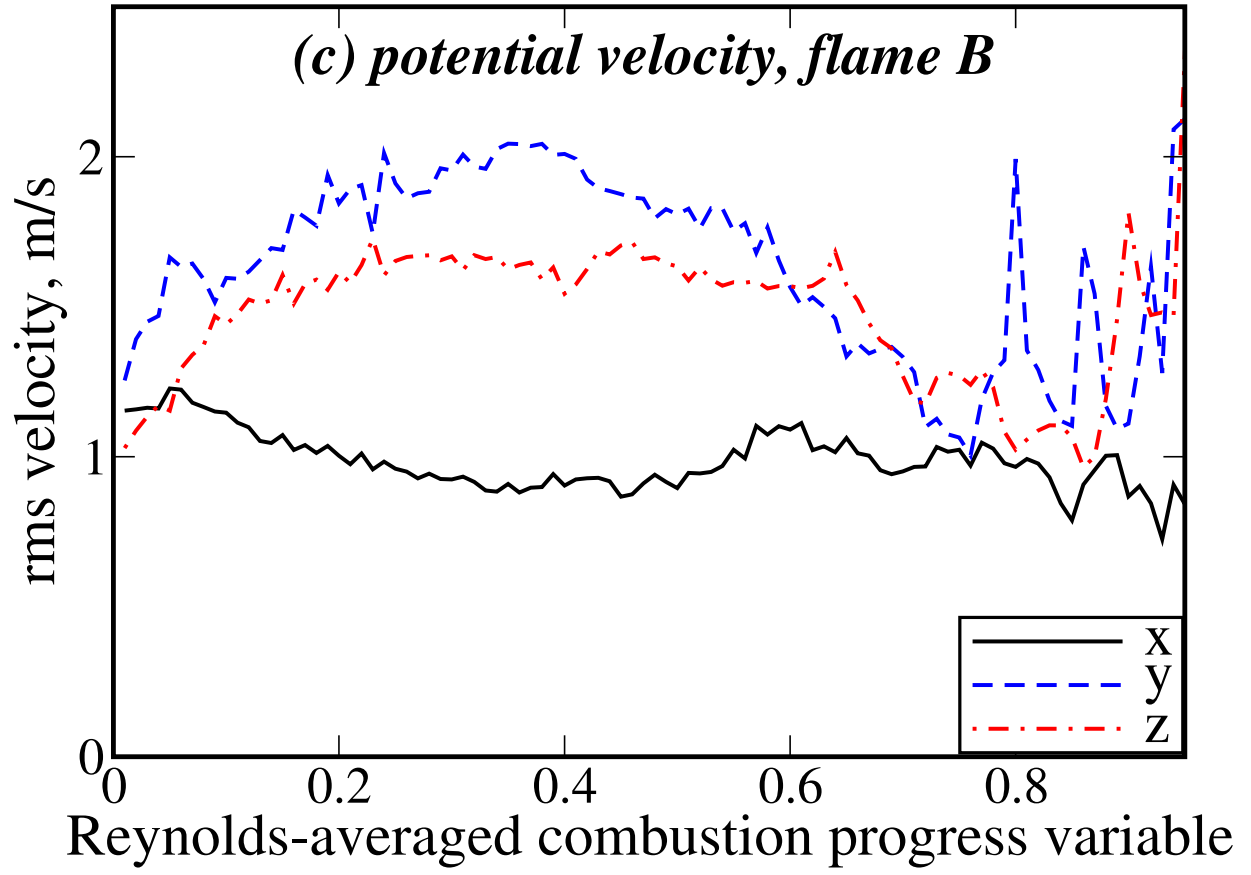
This is the author's peer reviewed, accepted manuscript. However, the online version of record will be different from this version once it has been copyedited and typeset.

PLEASE CITE THIS ARTICLE AS DOI: 10.1063/5.0123211



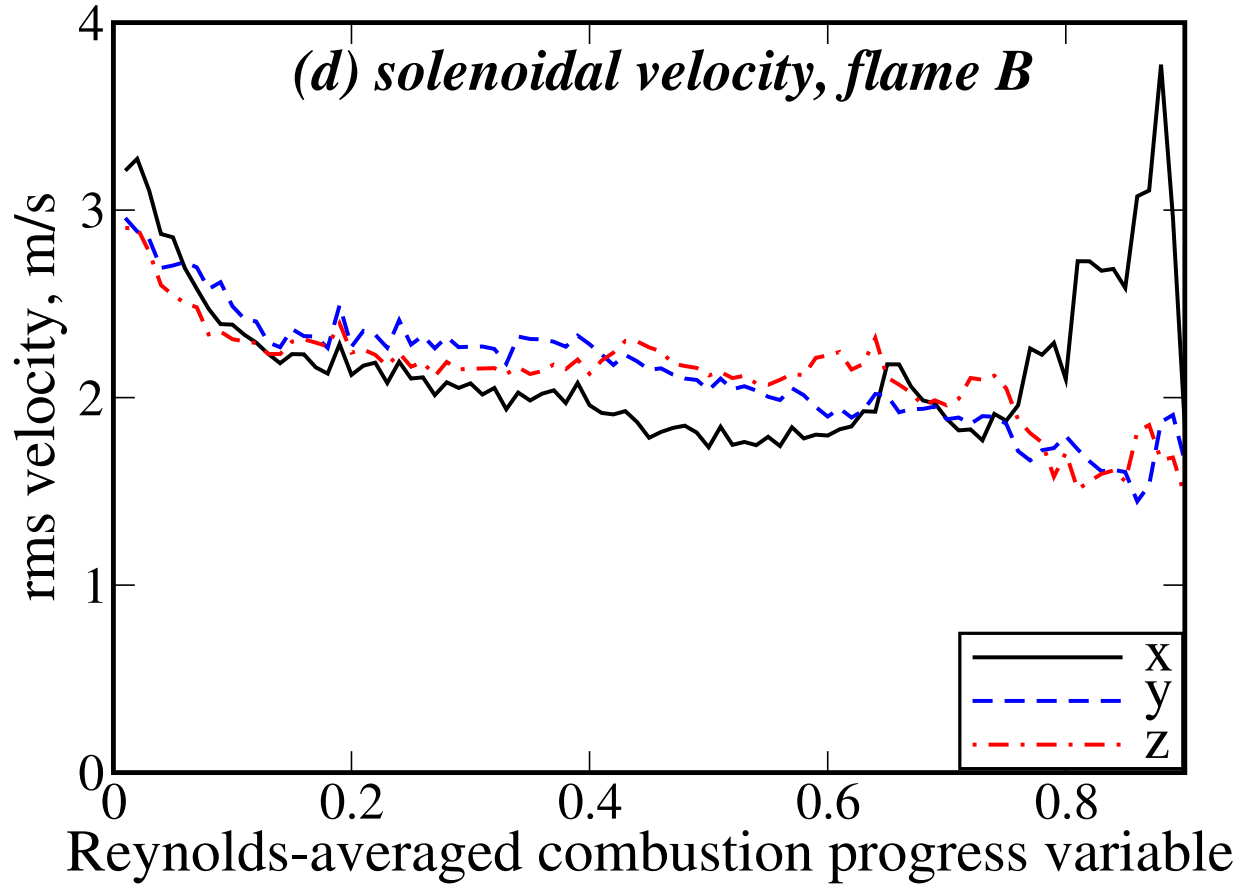
This is the author's peer reviewed, accepted manuscript. However, the online version of record will be different from this version once it has been copyedited and typeset.

PLEASE CITE THIS ARTICLE AS DOI: 10.1063/5.0123211



This is the author's peer reviewed, accepted manuscript. However, the online version of record will be different from this version once it has been copyedited and typeset.

PLEASE CITE THIS ARTICLE AS DOI: 10.1063/5.0123211



This is the author's peer reviewed, accepted manuscript. However, the online version of record will be different from this version once it has been copyedited and typeset.

PLEASE CITE THIS ARTICLE AS DOI: 10.1063/5.0123211

